Biochar

ORIGINAL RESEARCH

Open Access

Biochar potentially enhances maize tolerance to arsenic toxicity by improving physiological and biochemical responses to excessive arsenate

Md. Mezanur Rahman[1†], Ashim Kumar Das[2†], Sharmin Sultana[3], Protik Kumar Ghosh[4], Md. Robyul Islam[3], Sanjida Sultana Keya[1], Minhaz Ahmed[2], Sheikh Arafat Islam Nihad[5], Md. Arifur Rahman Khan[4], Mylea C. Lovell[1], Md. Abiar Rahman[2], S. M. Ahsan[6], Touhidur Rahman Anik[1], Pallavi Fnu[1], Lam-Son Phan Tran[1*] and Mohammad Golam Mostofa[7,8,9*]

Abstract

Metalloid pollution, including arsenic poisoning, is a serious environmental issue, plaguing plant productivity and quality of life worldwide. Biochar, a carbon-rich material, has been known to alleviate the negative effects of environmental pollutants on plants. However, the specific role of biochar in mitigating arsenic stress in maize remains relatively unexplored. Here, we elucidated the functions of biochar in improving maize growth under the elevated level of sodium arsenate (Na_2AsO_4, As^V). Maize plants were grown in pot-soils amended with two doses of biochar (2.5% (B1) and 5.0% (B2) biochar Kg^{-1} of soil) for 5 days, followed by exposure to Na_2AsO_4 ('B1 + As^V'and 'B2 + As^V') for 9 days. Maize plants exposed to As^V only accumulated substantial amount of arsenic in both roots and leaves, triggering severe phytotoxic effects, including stunted growth, leaf-yellowing, chlorosis, reduced photosynthesis, and nutritional imbalance, when compared with control plants. Contrariwise, biochar addition improved the phenotype and growth of As^V-stressed maize plants by reducing root-to-leaf As^V translocation (by 46.56 and 57.46% in 'B1 + As^V' and 'B2 + As^V' plants), improving gas-exchange attributes, and elevating chlorophylls and mineral levels beyond As^V-stressed plants. Biochar pretreatment also substantially counteracted As^V-induced oxidative stress by lowering reactive oxygen species accumulation, lipoxygenase activity, malondialdehyde level, and electrolyte leakage. Less oxidative stress in 'B1 + As^V' and 'B2 + As^V' plants likely supported by a strong antioxidant system powered by biochar-mediated increased activities of superoxide dismutase (by 25.12 and 46.55%), catalase (51.78 and 82.82%), and glutathione *S*-transferase (61.48 and 153.83%), and improved flavonoid levels (41.48 and 75.37%, respectively). Furthermore, increased levels of soluble sugars and free amino acids also correlated with improved leaf relative water content, suggesting a better osmotic acclimatization mechanism in biochar-pretreated As^V-exposed plants. Overall, our findings provided mechanistic insight into how biochar facilitates maize's active recovery from As^V-stress, implying

†Handling editor: Wenfu Chen.

Md. Mezanur Rahman and Ashim Kumar Das have equally contributed to this work.

*Correspondence:
Lam-Son Phan Tran
son.tran@ttu.edu
Mohammad Golam Mostofa
mostofam@msu.edu
Full list of author information is available at the end of the article

that biochar application may be a viable technique for mitigating negative effects of arsenic in maize, and perhaps, in other important cereal crops.

Highlights

- Maize developed significant growth defects under excessive arsenate (As^V) stress.
- Biochar addition decreased root As^V uptake and root-to-leaf As^V translocation.
- Biochar protected photosynthetic rate and pigment levels from As^V -stress.
- Biochar reduced As^V-caused oxidative damage by strengthening antioxidant defense.
- Biochar boosted osmoprotectant levels and nutrient uptake in As^V-stressed maize.

Keywords Arsenic contamination, Antioxidant defense system, Biochar, Gas-exchange attributes, Nutrient dynamics, Oxidative stress

Graphical Abstract

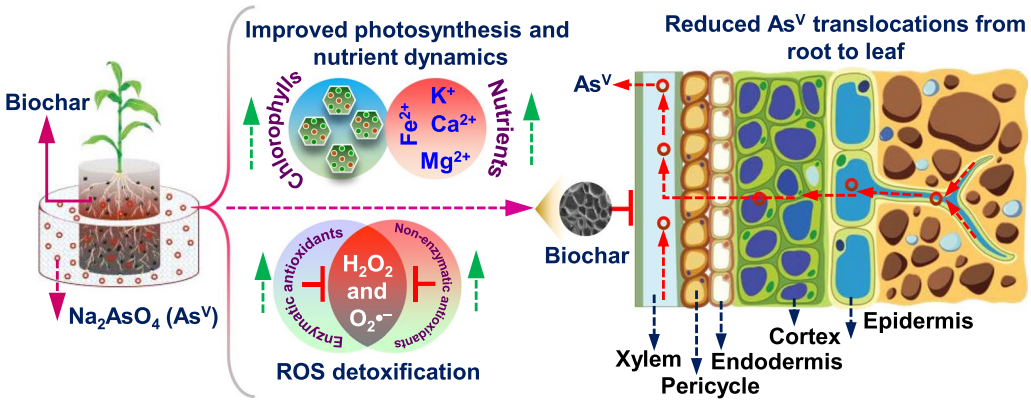

1 Introduction

Biochar, popularly alluded to as black gold in agriculture, is a carbon-rich organic material. It is manufactured from a wide range of feedstock, including crop residues, wood, animal manure, and other organic wastes (Khan et al. 2021; Liu et al. 2022a). Under oxygen-depleted conditions, a number of techniques, including slow/fast/microwave pyrolysis, traditional charcoal production, gasification, flash carbonization, and hydrothermal carbonization are employed for large scale production of biochar (Jiang et al. 2020). Biochar has received intense attention over the past decades for its remarkable potential to sequester carbon, reduce greenhouse gas emissions, and enhance soil quality through improvement of soil organic matter content, nutrient recycling, and water-holding capacity (Jiang et al. 2020; Xu et al. 2022a). Importantly, biochar can also remediate environmental contamination through its high sorption affinity for environmental pollutants (Kumar et al. 2022).

Environmental pollution with heavy metals and metalloids resulting from impromptu urbanization and industrial growth poses a significant threat to soil quality and crop yield worldwide (Gavrilescu 2022; Wang et al. 2022). Arsenic is one of the most prevalent natural elements and environmental toxicants. It is considered the most hazardous pollutant because of its carcinogenic properties, impacting the health of around 94 to 220 million people worldwide, with a majority (94%) located in Asia (Podgorski and Berg 2020; Bahrami et al. 2020; Roy et al. 2022). In fact, arsenic contamination has already been spread to approximately 64%, 14%, 10%, 9%, 2%, and 1% of the land area in Asia, South America, North America, Africa, Oceania, and Europe, respectively (Podgorski and Berg 2020). More fundamentally, arsenic concentrations in groundwater and drinkable water are higher than the World Health Organization's acceptable threshold of 10 μg L^{-1} in many developing countries, including Bangladesh (Rahaman et al. 2022). Concurrently, arsenic is the most hazardous metalloid for plant growth and

development when a considerable amount is absorbed from arsenic-contaminated environments (Bahrami et al. 2020; Mostofa et al. 2021a, b; Peña-Garcia et al. 2021). Two inorganic forms of arsenic, arsenite (As^{III}) and arsenate (As^{V}), predominantly exist in anaerobic and aerobic soils, respectively (Kandhol et al. 2022). Each can easily enter plant roots through distinct transportation systems. While plants use different types of aquaporin subfamilies to uptake As^{III}, As^{V} is transferred by phosphate (Pi)-transporters because of the structural similarity of As^{V} with Pi (Bahrami et al. 2020; Mostofa et al. 2021a, b). Arsenic, once accumulated in different parts of the plant body, impedes normal plant metabolism by interfering with sulfur, nitrogen, and carbon assimilation pathways (Finnegan and Chen 2012). Numerous physiological functions of plants, such as net photosynthetic rate, stomatal conductance, and transpiration rate, can be impacted by excessive arsenic (Srivastava et al. 2015). Furthermore, arsenic accumulation in cells can result in the overproduction of reactive oxygen species (ROS), leading to oxidative damage to cellular constituents, such as proteins, enzymes, nucleic acids, and lipids (Abbas et al. 2018).

Plants use a variety of defense mechanisms to combat arsenic toxicity, for example restraining arsenic uptake and transportation by downregulating arsenic transport and translocation mechanisms, synthesizing arsenic-chelating metabolites like glutathione and phytochelatins, strengthening antioxidant defense, and sequestering arsenic into vacuoles (Dixit et al. 2016; Begum et al. 2016; Mostofa et al. 2021a, b; Vezza et al. 2019). Currently, different strategies, including ion-exchange, adsorption, chemical precipitation, and phytoremediation are in practice to remove arsenic from arsenic-contaminated soils and water (Alka et al. 2021). While chemical precipitation and ion-exchange provide maximum efficiency, their implementation demands substantial energy, economic input, and routine maintenance (Ahmed 2001; Ali et al. 2013; Hu and Boyer 2018; Senn et al. 2018). Although phytoremediation is eco-friendly, its applicability for broader spectrum is restrained by its time-consuming nature (Gavrilescu 2022; Yan et al. 2020). Adsorption techniques like the application of minerals, activated carbon, fly ash, biochar, and graphene are frequently employed nowadays to remove arsenic from contaminated water and soils (Sun et al. 2022). Due to its abundant supply, cost-effectiveness, ease of use, and ecologically favorable qualities, the utilization of biochar has emerged as an excellent strategy to protect plants from the toxicity of different environmental pollutants, including arsenic (Sun et al. 2022; Zama et al. 2022). Indeed, because of the discrepancies in adsorption characteristics resulting from diverse raw materials and production conditions in biochar manufacturing, a single type of biochar cannot holistically eradicate all heavy metals from contaminated sources. Consequently, a wealth of research now focuses on the modification of physicochemical properties of biochar to bolster its adsorption capacity and selective affinity for contaminants (Cheng et al. 2021). This optimization predominantly relies on diverse factors, including mineral composition, pH levels, temperature, biochar quantity, adsorption duration, and pollutant characteristics (Qiu et al. 2021; Srivastav et al. 2021).

Maize (*Zea mays*), which ranks the third among cereals only after wheat and rice, is grown for human food and animal feed on a global scale. (De Feudis et al. 2019; Yin et al. 2021). Nonetheless, the industrial evolution and long-term wastewater irrigation lead to heavy metals and metalloid buildup in soils used to cultivate important crops like maize. Excessive arsenic contamination ultimately results in poor maize growth and development, as well as increased contents of arsenic in their grains (Ben Fredj et al. 2013; Rashid et al. 2022; Rizvi et al. 2022; Romdhane et al. 2021; Xu et al. 2022b; Zheng et al. 2019). Considering its effective roles in heavy metal-toxicity mitigation, biochar application could be a straightforward, less time-consuming, and cost-effective way to protect maize plants from the damaging effects of arsenic. Thus, the present study aimed at evaluating whether or not biochar restricts arsenic accumulation and translocation in maize roots and shoots and, if it does so, determining the underlying mechanism of that restriction. We were particularly interested in discovering how biochar application modulates key physiological and biochemical mechanisms that are associated with arsenic accumulation, gas exchange features, photosynthetic performance, osmoprotection, and antioxidant defense mechanisms in maize plants subjected to excessive arsenate-stress.

2 Materials and methods

2.1 Biochar production: sourcing, preparation, and characterization

Bangladesh is ranked the fourth among the world's largest rice-producing countries, yielding approximately 34.70 million metric tons of rice annually from 11.75 million hectares land (IRRI 2021). Consequently, a substantial amount of rice byproducts, including rice husks, are being generated, which could be used to produce value-added products like biochar. In this study, fresh rice husk was procured from a local rice mill and used for biochar production by pyrolyzing rice husk at 400 to 550 °C without oxygen using a customized pyrolysis stove designed by the Soil Science Department of Bangabandhu SMR Agricultural University, Bangladesh (Hasnat et al. 2022). After completing pyrolysis, the heated biochar was

quenched with distilled water, followed by sun-drying before being powdered into fine particles (< 2 mm). The resultant biochar was also analyzed to determine its key physical and chemical properties (Additional file 1: Table S1). Briefly, total N percentage in biochar was determined following the Kjeldahl method described by Jackson (1973). The percentage of exchangeable K, Zn, Ca, Mg, Cu, and Mn in biochar was determined following the detailed procedures of Piper (1966). Organic carbon (OC) content was quantified according to the wet oxidation method (Walkley and Black 1934). In addition, the pH of the rice husk biochar solution was measured using HANNA HI 8424 pH meter.

The point of zero charge (pHpzc) for biochar was determined utilizing five conical flasks (250 mL). Each flask contained 50 mL of 0.1 M NaCl solution and 0.1 g of biochar. Subsequently, the pH of the solution was systematically adjusted to 2.0, 4.0, 6.0, 8.0, and 10.0 by adding either 0.1 M HCl or NaOH solution. Subsequent to 24 h of stirring, the supernatant was separated, and its pH level was measured. The pHpzc value was derived by plotting the initial pH of the solution against the pH of the supernatant (final pH after 24 h). To evaluate surface morphologies, a delicate layer of gold was applied to the biochar samples. These samples underwent analysis using a JCM-7000 NeoScope™ Benchtop Scanning Electron Microscope (SEM, JEOL, Japan), operating at 15 kV. The metallization of the samples was conducted using a Smart Coater (DII-29030SCTR, JEOL, Japan), at the Plant Pathology Division of the Bangladesh Rice Research Institute (BRRI), Gazipur, Bangladesh. The acquired SEM images and data for Energy-dispersive X-ray spectroscopy (EDS) analysis were obtained through the official JEOL software (JEOL, Tokyo, Japan).

2.2 Experimental design and treatment compositions

The biochar was mixed with the previously prepared soil (3:1; soil: cow dung on a weight basis) at the rate of 0, 2.5, and 5.0% Kg^{-1} of soil, respectively. The biochar doses were chosen based on the results from an initial experiment (Additional file 1: Fig. S1). Five days after biochar amendment, eight seeds of a high-yielding (11.5–12.5 tons ha^{-1}) maize (BARI Hybrid Maize-9) variety were directly sown in one L plastic pots (11 cm in height and 12.5 cm in diameter) containing 700 g of biochar-mixed soil. After seedling establishment, the number of seedlings in pot^{-1} was thinned to five. Pots containing five-day-old plants were then placed in white plastic pots (6.5 cm in height and 13.5 cm in diameter) (Fig. 1). Afterward, 700 mL of either tap water or sodium arsenate (Na_2AsO_4, As^V) solution was poured into white plastic pots to saturate the soil (Fig. 1). Based on the results from the initial experiment, the As^V-dose (100 mg Kg^{-1} soil) was chosen (Additional file 1: Fig. S2). Importantly, the volume of tap water or As^V solution in white plastic pots was constantly maintained throughout the experimental period to ensure that the uptake of the solution through the plant's root system resembled that of natural environments. Overall, there were six different treatments in our experiment: (i) Control (Ctrl), (ii) 2.5% biochar Kg^{-1} of soil (B1), (iii) 5.0% biochar Kg^{-1} of soil (B2), (iv) 100 mg Na_2AsO_4 Kg^{-1} of soil (As^V), (v) B1 + As^V, and (vi) B2 + As^V. Nine days after As^V exposure, the second leaf (from the bottom) of the fourteen-day-old maize plants was excised to examine numerous parameters related to maize morphology, physiology, and cellular biochemistry. After As^V exposure, the chemical properties of soil were also recorded (Additional file 1: Table S2). Most importantly, we also quantified the arsenic content in soil under different treatment compositions, as well as in the biochar (Additional file 1: Table S3). To confirm the reliability of the results, we performed the experiment three times.

2.3 Quantification of As^V and mineral contents

Leaf and root (0.1 g) samples were oven-dried and pulverized before being digested in a DK 8S Heating digester machine (Velp Scientifica, NY 11729, USA) with 5 mL of a nitric acid: perchloric acid solution (5:1, v/v) for 2.5 h at 190 °C. Afterward, deionized water was added to the digested samples to raise their volume to 100 mL and filtered using Whatman filter paper (Grade 42). From this 100 mL, 5 mL of solution was withdrawn, and the final volume was brought up to 50 mL by adding deionized water. The contents of As^V, calcium (Ca^{2+}), potassium (K^+), iron (Fe^{2+}), and magnesium (Mg^{2+}) were determined using atomic absorption spectrophotometer PinAAcle 900H (Perkin Elmer Company, Waltham, MA, USA). The As^V translocation factor (TF) within various plant parts was determined using the following formula reported by Mostofa et al. (2017), with minor changes:

TF = As^V content in leavess/ As^V content in roots.

2.4 Root and shoot growth assays

After nine days of As^V-stress, plants were carefully uprooted from each pot and rinsed with distilled water to eliminate adhered soils. Next, the maize plant's primary root length and shoot height were measured using a measuring scale. Roots and shoots were subsequently separated, and the root volume of maize plants was determined by immersing washed roots in a measuring cylinder. The increased volume of water was recorded and expressed as g mL^{-1} (Islam et al. 2020). Roots and shoots were then oven-dried at 70 °C for 72 h to estimate dry weight (DW). The maize plant's individual leaf area

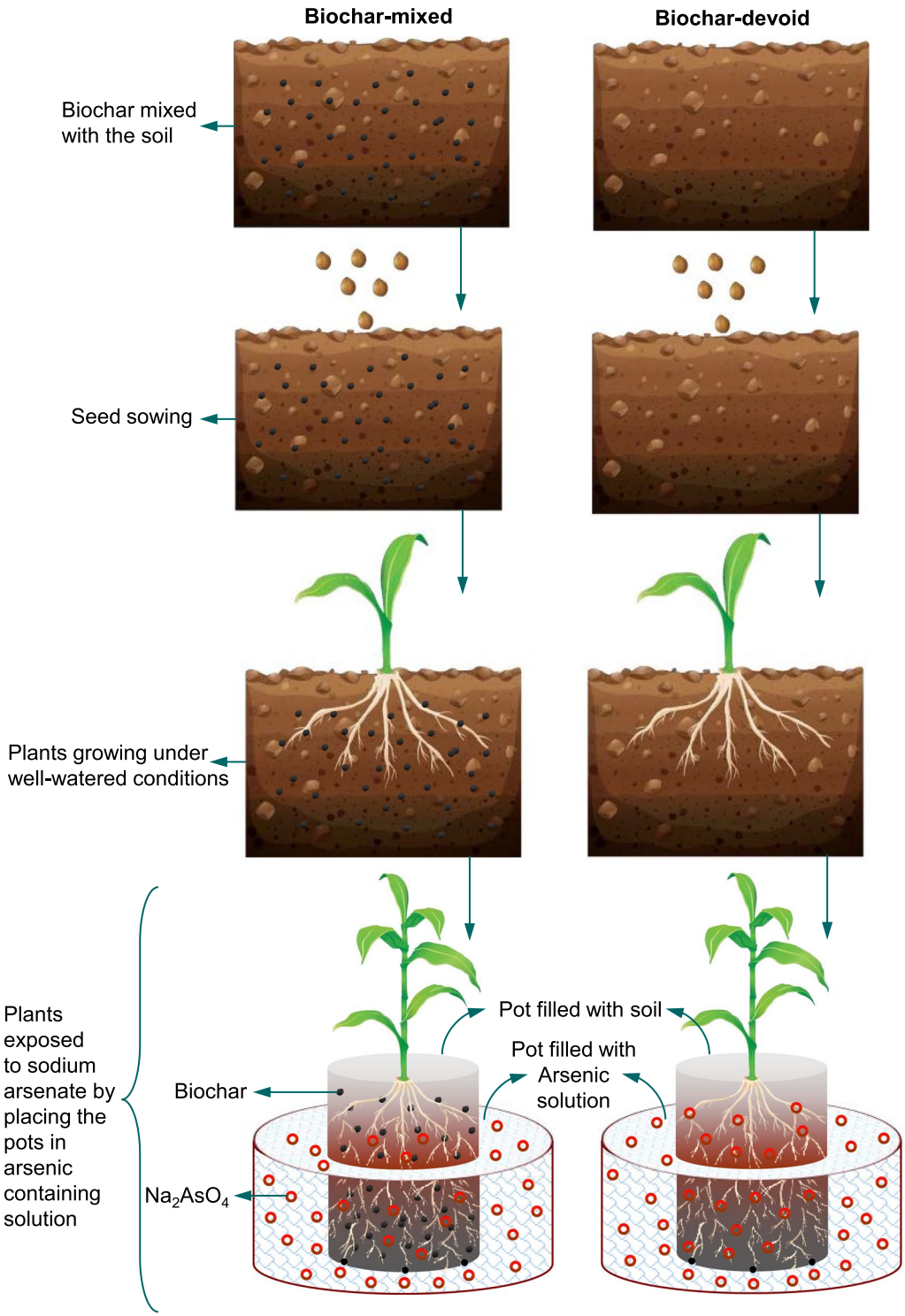

Fig. 1 Representative diagram of experimental design

was determined using the equation stated by Rahman et al. (2022).

2.5 Quantification of chlorophylls and carotenoids

Chlorophyll (Chl) *a*, Chl *b*, total Chls, and carotenoids in 80% (v/v) acetone-extracted supernatant were quantified by recording the absorbance at A_{663}, A_{645}, and A_{470} nm using a GENESYS 10S spectrophotometer (Thermo Scientific, San Jose, CA, USA). The equations of Arnon (1949), and Lichtenthaler and Wellburn (1983) were used to determine Chl and carotenoid levels, respectively.

2.6 Assessment of photosynthetic rate, transpiration rate, leaf temperature, and stomatal conductance

A portable LI-6400XT photosynthesis measurement system manufactured by LI-COR Biosciences (Lincoln, NE) was used to determine the rate of photosynthesis (P_n), transpiration (E), stomatal conductance (g_s), and leaf temperature (LT) in the middle portion of the 2nd leaf (from the bottom) of four randomly chosen plants from each treatment group.

2.7 Detection of reactive oxygen species in leaves and quantifications of H_2O_2 and MDA levels, and EL percentage

The accumulation of superoxide ($O_2^{\bullet-}$) and hydrogen peroxide (H_2O_2) in maize leaves was visually detected following histochemical staining techniques using nitro blue tetrazolium (NBT) and diaminobenzidine (DAB), respectively, as described by Das et al. (2022). Furthermore, spectrophotometric quantification of H_2O_2 and malondialdehyde (MDA) was carried out according to the procedures proposed by Yu et al. (2003) and Kim et al. (2020), respectively. Electrolyte leakage (EL) in maize leaves was determined using an electrical conductivity meter following the procedure reported by Rahman et al. (2022).

2.8 Determination of enzymatic antioxidant activities, LOX activity, and the levels of total flavonoids

Enzyme extraction and activities of glutathione *S*-transferase (GST), catalase (CAT), glutathione peroxidase (GPX), superoxide dismutase (SOD), ascorbate peroxidase (APX), and peroxidase (POD) in maize leaves were evaluated as explained by Rahman et al. (2019). On the other hand, the activity of monodehydroascorbate reductase (MDHAR), glutathione reductase (GR), and dehydroascorbate reductase (DHAR), was assessed following protocols described by Hossain et al. (1984), Foyer and Halliwell (1976), and Nakano and Asada (1981), respectively. The lipoxygenase (LOX) activity was measured following oxidation of linoleic acid by monitoring the change in absorbance at 234 nm, as described by Boyes et al. (1992).

The contents of protein and total flavonoids were estimated following the methods defined by Bradford (1976) and Das et al. (2022), respectively.

2.9 Determination of leaf RWC, Pro, TSS, TFAA, and total carbohydrates

The method of Das et al. (2022) was adopted to determine relative water content (RWC) in maize leaves. Next, proline (Pro) level was determined following Bates et al. (1973) method using an acid ninhydrin-based procedure. The protocols described by Somogyi (1952), and Lee and Takahashi (1966) were followed to determine the total soluble sugar (TSS) and total free amino acids (TFAA) levels, respectively. The procedure of Dubois et al. (1956) was adopted to assess the level of total carbohydrates.

2.10 Statistical analysis

Statistix 10 software was used to conduct a one-way analysis of variance to identify the interactive effects of biochar and As^V toxicity in maize seedlings. Variations within treatments were analyzed using least significant difference tests at a significance level of $P < 0.05$. Means and standard errors (SEs) of three (for arsenic content, antioxidant enzymes, leaf osmoprotectant, and ion estimation) and four (for morphological features, gas-exchange features, photosynthetic pigments, and oxidative stress markers) replicates per treatment were plotted graphically.

3 Results

3.1 Characterization of rice husk biochar through scanning electron microscopy (SEM) and elucidation of its pH-related effects

The examination of rice husk biochar using SEM revealed that biochar's surface morphology was highly diverse and complex, as characterized by a multitude of pores of varying diameters (Fig. 2A–F). Importantly, our Energy-dispersive X-ray spectroscopy (EDS) analysis revealed that biochar devoid of As^V exposure displayed a composition comprised of oxygen and silicon elements. Intriguingly, the addition of biochar samples with As^V solution, followed by 24 h of stirring, meticulous filtration, and subsequent EDS analysis revealed that, apart from oxygen and silicon elements, arsenic was also present (Fig. 2G–N). This intriguing finding strongly implies the ability of biochar to adsorb arsenic species from its surrounding environment. Indeed, the pH of the solution exerted influence over the surface charge of the adsorbent, as well as the extent of ionization and the configuration of surface functional groups. Our analysis revealed that the zero-point charge (pHzpc) of rice husk biochar was around 6.8 (Additional file 1: Fig. S3). At pH values lower than the pHzpc, the adsorbent's surface carried a positive

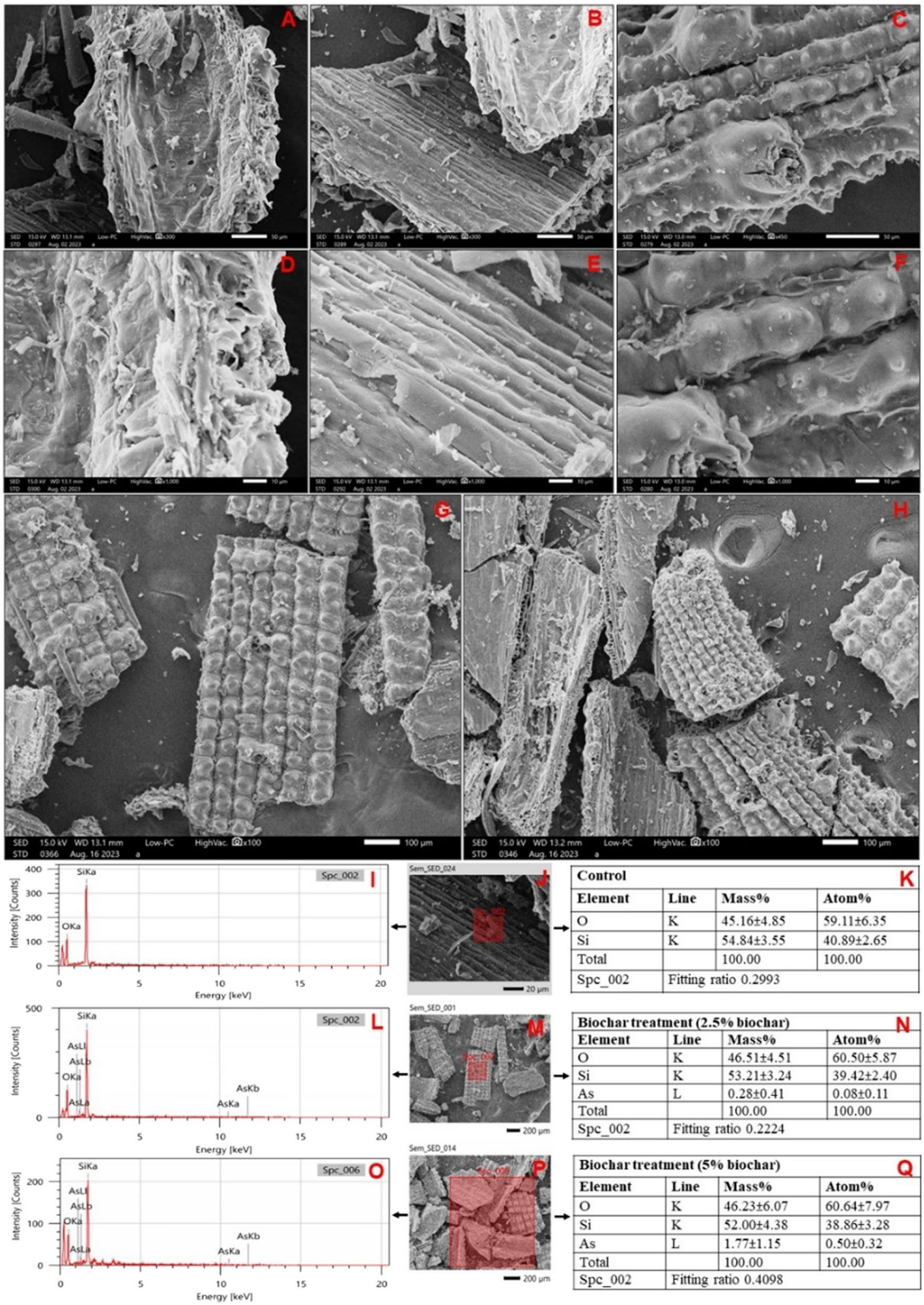

Fig. 2 Scanning Electron Microscope view of rice biochar samples. **A–F** Different structures of biochar under SEM at different magnification (×300, 450, and 1000) without As^V exposure. **G** 2.5% of biochar mixed with As^V solution (×100 magnification), **H** 5% of biochar mixed with As^V solution. (**I**–**K**) Energy-dispersive X-ray spectroscopy (EDS) analysis report of biochar without As^V solution, (**L**–**N**) 2.5% biochar with As^V solution, and (**O**–**Q**) 5.0% biochar with As^V solution (**O**–**Q**)

charge owing to the presence of H^+ ions. Whereas, at pH levels surpassing the pHzpc, the surface became negatively charged due to the presence of hydroxyl ion (OH^-).

3.2 Biochar addition improved phenotypic appearance and maintained arsenic homeostasis under As^V-stress conditions in maize plants

Maize plants exposed to As^V-stress for nine days displayed severe phenotypic disorders, including arrested growth, yellowing of lower leaves, burnt leaf tips, and inhibited root proliferation (Fig. 3A, B). Intriguingly, compared with the 'As^V' plants, biochar pretreatment substantially improved the phenotypic appearance of '$B1+As^V$' and '$B2+As^V$' plants, indicating that the As^V-induced phytotoxic effects were mitigated (Fig. 3A, B). Additionally, biochar pretreatment improved the phenotypic appearance, particularly root growth in 'B1' and 'B2' plants, in relation to 'Ctrl' plants (Fig. 3A, B). To examine the restorative effects of biochar, a group of plants was subjected to five days of As^V-stress followed by consistent irrigation for five days. The results indicated that biochar-treated As^V-stressed plants recovered better than the As^V-stressed plants only, highlighting the roles of biochar in active recovery of maize plants from As^V-stress (Additional file 1: Fig. S4).

To uncover the underlying cause of phenotypic alterations, we quantified the arsenic concentration in roots and leaves (Fig. 3C, D). In comparison with 'Ctrl' plants, arsenic concentration in roots and leaves was substantially increased by 9,391.90 and 28,060.78%, respectively, in 'As^V' plants (Fig. 3C, D). By comparison, biochar pretreatment significantly reduced arsenic content by 49.06 and 64.63% in roots, and 72.16 and 84.77% in leaves of '$B1+As^V$' and '$B2+As^V$' plants, respectively, when compared with 'As^V' plants (Fig. 3C, D). However, in the absence of As^V, 'B1' and 'B2' plants exhibited comparable levels of arsenic in roots and leaves (Fig. 3C, D). More fundamentally, compared with control, translocation of As^V from root-to-leaf increased by 199.68% in 'As^V' plants (Fig. 3E). Contrariwise, biochar supplementation reduced the translocation of As^V from root-to-leaf by 46.56 and 57.46% in '$B1+As^V$' and '$B2+As^V$' plants, respectively, when compared with 'As^V' plants (Fig. 3E). These findings suggested that under As^V-stress conditions, biochar pretreatment had a better alleviatory effect on the phenotype, as well as in the uptake of As^V in maize plants; the betterment was more prominent in '$B2+As^V$' plants than '$B1+As^V$'plants.

3.3 Biochar application enhanced growth performance in As^V-stressed maize plants

In comparison with 'Ctrl' plants, 'As^V' plants showed considerable reduction in primary root length by 50.21%, shoot height by 14.75%, root dry weight by 60.59%, shoot dry weight by 46.98%, root volume by 65%, and individual leaf area by 16.37% (Fig. 4A–F). On the other hand, in relation to 'As^V' plants, pretreatment of plants with biochar notably improved root length by 35.99% and 34.70%, shoot height

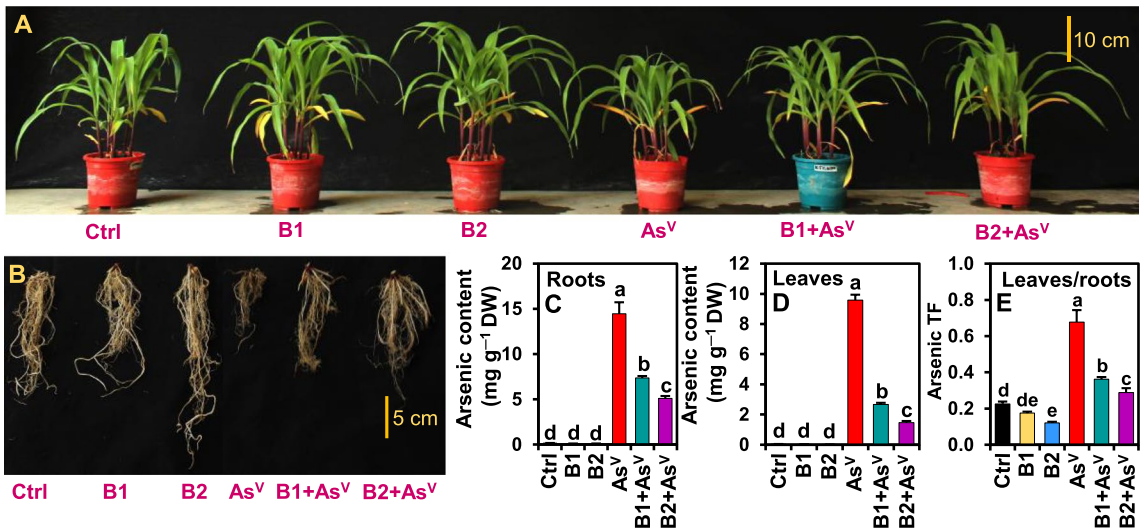

Fig. 3 Phenotypic changes of (**A**) shoot and (**B**) root of maize plants subjected to sodium arsenate (Na_2AsO_4, As^V) stress for nine days with and without biochar. Effect of biochar on total arsenic accumulation in (**C**) roots and (**D**) leaves, and (**E**) arsenic TF from roots to leaves of maize plants grown under As^V-stress conditions. Numerical data presented here indicates means ± standard errors of three biological repeats. LSD test determines significant differences (at $P < 0.05$) between treatments by different alphabetical letters. Ctrl, B1, B2, As^V, B1 + As^V and B2 + As^V indicate 0 mg As^V Kg^{-1} soil, 2.5% biochar-added soil, 5.0% biochar-added soil, 100 mg As^V Kg^{-1} soil, 2.5% biochar-added soil + 100 mg As^V Kg^{-1} soil, and 5.0% biochar-added soil + 100 mg As^V Kg^{-1} soil, respectively. *DW* dry weight, *LSD* least significant difference, *TF* translocation factor

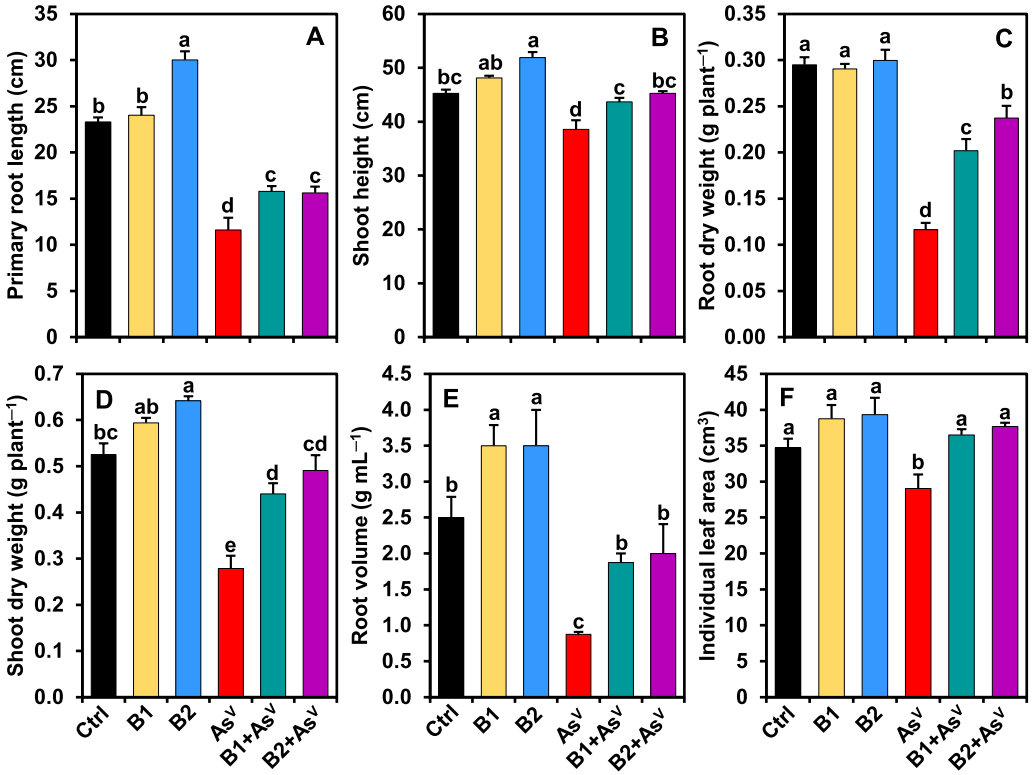

Fig. 4 Effect of biochar on (**A**) primary root length, (**B**) shoot height, (**C**) root dry weight, (**D**) shoot dry weight, (**E**) root volume, and (**F**) individual leaf area of maize plants subjected to sodium arsenate (Na_2AsO_4, As^V) for a period of nine days. Numerical data presented here indicate means ± standard errors of four biological repeats. LSD test determines the significant differences (at $P < 0.05$) between treatments by different alphabetical letters. Ctrl, B1, B2, As^V, B1 + As^V and B2 + As^V indicate 0 mg As^V Kg^{-1} soil, 2.5% biochar-added soil, 5.0% biochar-added soil, 100 mg As^V Kg^{-1} soil, 2.5% biochar-added soil + 100 mg As^V Kg^{-1} soil, and 5.0% biochar-added soil + 100 mg As^V Kg^{-1} soil, respectively. *LSD* least significant difference

by 13.22 and 17.37%, root dry weight by 73.76 and 104.09%, shoot dry weight by 57.99 and 76.30%, root volume by 114.29% and 128.57%, and individual leaf area by 25.70% and 29.75% in 'B1 + As^V' and 'B2 + As^V' plants, respectively (Fig. 4A–F). Moreover, supplementation of biochar to As^V-treated plants significantly enhanced primary root length by 28.86%, shoot height by 14.64%, and shoot dry weight by 22.13% in 'B2' plants, when compared with 'Ctrl' plants (Fig. 4A, B, D). However, in relation to 'Ctrl' plants, 'B1' and 'B2' plants displayed noteworthy enhancement of root volume by 40% of each, respectively (Fig. 4E). The findings also indicated that biochar pretreated 'B2 + As^V' plants displayed better improvement in root and shoot height, dry weight, and root volume, as well as in individual leaf area under As^V-stress conditions.

3.4 Biochar application improved photosynthetic pigment content, stomatal conductance to water, and transpiration rate but declined leaf temperature in As^V-stressed maize plant

'As^V' plants displayed considerable declines in P_n by 33.70%, E by 61.02%, g_s by 59.36%, as well as the levels of Chl *a* by 39.67%, Chl *b* by 41.45%, total Chls by 40.34%, and carotenoids by 36.13%, when compared with the 'Ctrl' plant (Fig. 5A, B, D, E–H). However, LT between 'As^V' and 'Ctrl' plants did not show any significant divergence (Fig. 5C). In comparison with 'As^V' plants, stressed plants supplemented with biochar showed a significant increase in P_n by 76.52 and 135.81%, E by 172.66 and 537.45%, g_s by 70.67 and 199.23%, and the content of Chl *a* by 38.74 and 12.96%, Chl *b* by 45.43 and 56.33%, total Chls by 41.22 and 56.58%, while decreasing LT by 3.12 and 5.13%, in 'B1 + As^V' and 'B2 + As^V' plants, respectively (Fig. 5A–G). Moreover, 'B2 + As^V' plants displayed significant enhancement of carotenoid content by 39.22% in relation to 'As^V' plants (Fig. 5H). In contrast to 'Ctrl' plants, 'B1' and 'B2' plants showed noteworthy enhancement in P_n by 66.98 and 95.14%, E by 180.80 and 242.52%, and g_s by 73.58 and 74.06%, while exhibiting a decrease in LT by 15.50 and 15.92%, respectively (Fig. 5A–D). On the other hand, the content of Chl *a*, Chl *b*, total Chls, and carotenoids were significantly elevated by 33.76, 49.86, 39.85, and 35.51%, respectively, in 'B2' plants, as compared with that of 'Ctrl' plants (Fig. 5E–H). However,

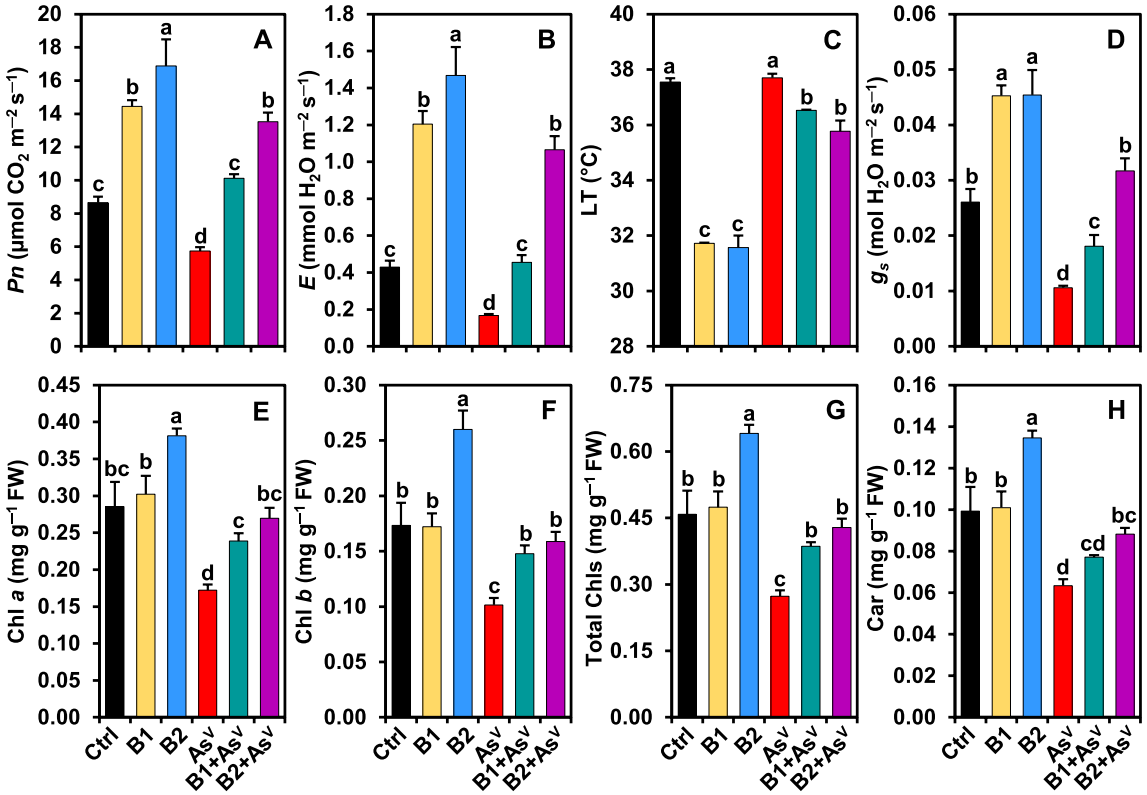

Fig. 5 Effect of biochar on (**A**) P_n, (**B**) *E*, (**C**) LT, (**D**) g_s, (**E**) Chl *a*, (**F**) Chl *b*, (**G**) total Chl, and (**H**) Car of maize plants subjected to sodium arsenate (Na_2AsO_4, As^V) stress for a period of nine days. Numerical data presented here indicate means ± standard errors of four biological repeats. LSD test determines the significant differences (at $P < 0.05$) between treatments by different alphabetical letters. Ctrl, B1, B2, As^V, B1 + As^V and B2 + As^V indicate 0 mg As^V Kg^{-1} soil, 2.5% biochar-added soil, 5.0% biochar-added soil, 100 mg As^V Kg^{-1} soil, 2.5% biochar-added soil + 100 mg As^V Kg^{-1} soil, and 5.0% biochar-added soil + 100 mg As^V Kg^{-1} soil, respectively. *Chl* chlorophyll, *Chl a* chlorophyll *a*, *Chl b* chlorophyll *b*, *Car* carotenoids, *E* transpiration rate, *FW* fresh weight, g_s stomatal conductance to water, *LT* leaf temperature, *LSD* least significant difference, P_n net photosynthetic rate

we did not observe any noteworthy differences in levels of photosynthetic pigments between 'Ctrl' and 'B1' plants (Fig. 5E–H). These results made it apparent that pretreating the maize plant with biochar at both concentrations modulated gas exchange features, as well as protected photosynthetic pigments under As^V-stress. Overall, 'B2 + As^V' plants performed better than 'B1 + As^V' plants.

3.5 Biochar supplementation minimized LOX activity and reduced H_2O_2, MDA, and electrolyte leakage levels

The accumulation of $O_2^{\bullet-}$ and H_2O_2 was visualized by staining the second leaf blades of maize plants with NBT and DAB, respectively. In contrast to 'Ctrl' leaves, 'As^V' leaves displayed dark blue and dark brown polymerization spots, indicating overproduction of $O_2^{\bullet-}$ and H_2O_2, respectively (Fig. 6A, B). Contrarily, compared with 'As^V' leaves, the addition of biochar significantly reduced production of excess $O_2^{\bullet-}$ and H_2O_2 in 'B1 + As^V' and 'B2 + As^V' leaves (Fig. 6A, B). Compared with 'Ctrl' plants, maize plants exposed to 'As^V' stress substantially increased the levels of H_2O_2 by 114.99%, MDA by 262.72% and EL by 523.52%, and LOX activity by 410.88% (Fig. 6C–F). Biochar supplementation, on the other hand, reduced the levels of H_2O_2 by 30.12 and 43.61%, MDA by 44.91 and 57.46% and EL by 51.04 and 65.05%, and LOX activity by 45.99 and 58.90%, in 'B1 + As^V' and 'B2 + As^V'plants, respectively, when equated with 'As^V' plants (Fig. 6C–F). Without As^V-stress, leaves of 'Ctrl' and 'B1', and 'B2' plants displayed equivalent levels of H_2O_2, MDA and EL, and LOX activity (Fig. 6C–F). According to these results, biochar pretreatment has an effective impact on the reducing levels of H_2O_2, MDA and EL, and LOX activity in maize plants under As^V stress conditions; the improvement was more pronounced in 'B2 + As^V' plants than in 'B1 + As^V' plants.

3.6 Biochar treatment upregulated enzymatic antioxidants to overcome As^V-induced oxidative stress

Compared with As^V-free 'Ctrl' plants, activities of SOD and CAT were substantially improved by 131.34 and 93.13%, respectively, in 'As^V' plants (Fig. 7A, B). Maize plants pretreated with biochar exposed to arsenic

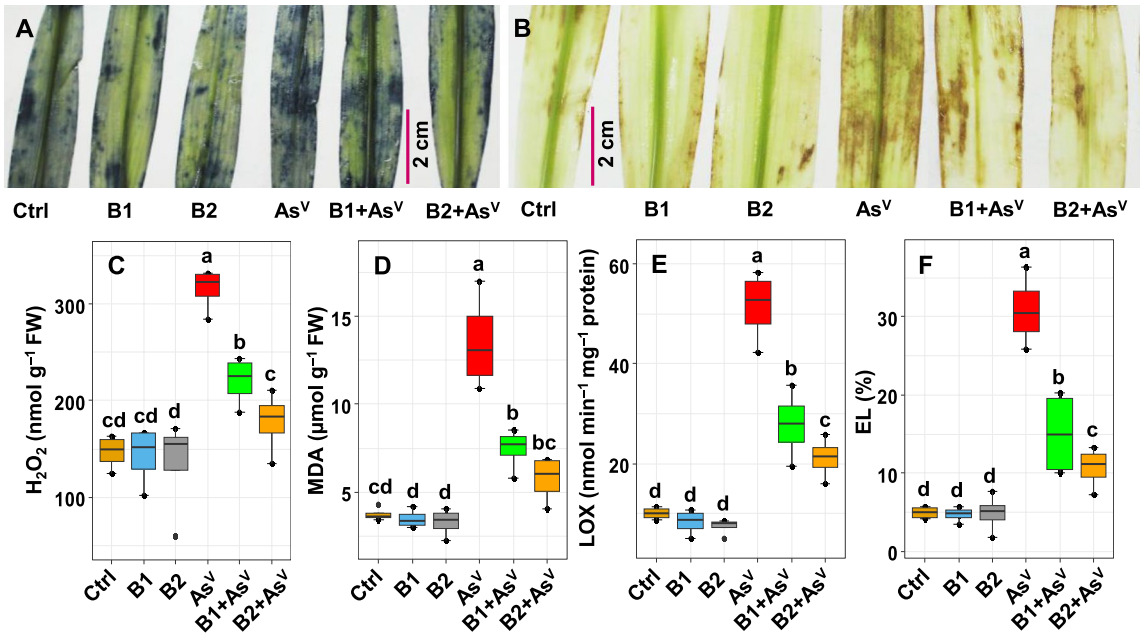

Fig. 6 Effect of biochar on ROS accumulation, levels of MDA and EL, and LOX activity in the leaves of maize plants subjected to sodium arsenate (Na_2AsO_4, As^V) for a period of nine days. Visual detection of (**A**) $O_2^{\bullet-}$ and (**B**) H_2O_2 by histochemical staining with NBT and DAB, respectively. Estimation of (**C**) H_2O_2, (**D**) MDA, (**E**) LOX activity, and (**F**) EL levels in leaves of maize plants. Numerical data presented here indicate means ± standard errors of four biological repeats. LSD test determines the significant differences (at $P < 0.05$) between treatments by different alphabetical letters. Ctrl, B1, B2, As^V, B1 + As^V and B2 + As^V indicate 0 mg As^V Kg^{-1} soil, 2.5% biochar-added soil, 5.0% biochar-added soil, 100 mg As^V Kg^{-1} soil, 2.5% biochar-added soil + 100 mg As^V Kg^{-1} soil and 5.0% biochar-added soil + 100 mg As^V Kg^{-1} soil, respectively. *DAB* diaminobenzidine, *EL* electrolyte leakage, *FW* fresh weight, H_2O_2 hydrogen peroxide, *LOX* lipoxygenase, *LSD* least significant difference, *MDA* malondialdehyde, *NBT* nitroblue tetrazolium, $O_2^{\bullet-}$ superoxide, *ROS* reactive oxygen species

stress significantly improved the activities of SOD by 25.12 and 46.55%, and CAT by 32.66 and 67.70%, in 'B1 + As^V' and 'B2 + As^V' plants, respectively, when contrasted with 'As^V' plants (Fig. 7A, B). Moreover, biochar applications to arsenic-devoid plants also displayed substantial improvement in the activities of SOD by 125.24 and 168.61%, and CAT by 51.78 and 82.82%, in 'B1' and 'B2' plants, respectively, as compared with that of 'Ctrl' plants (Fig. 7A, B). The activity of AsA-GSH cycle enzymes POD, APX, MDHAR, DHAR, and GR, were also evaluated in maize leaves under AsV-stress conditions, with and without biochar (Fig. 7C–G). In comparison with 'Ctrl' plants, 'As^V' plants displayed significant improvement in activities of POD, APX, MDHAR, DHAR, and GR by 32.74, 83.88, 187.57, 214.53, and 140.11%, respectively (Fig. 7C–G). 'B1 + As^V' and 'B2 + As^V' plants, on the other hand, exhibited increased activities of MDHAR (by 33.30 and 194.68%), DHAR (by 142.24 and 314.26%), and GR (by 221.26 and 240.37%, respectively), as compared with 'As^V' plants (Fig. 7E–G). However, there were no discernible differences in APX and POD activities between 'As^V' and 'B1 + As^V' plants while 'B2 + As^V' plants showed a significant increase in POD activity by 56.08% and APX activity by 100.70%, in comparison to 'As^V' plants (Fig. 7C, D). Additionally, compared with 'Ctrl' plants, 'B1' and 'B2' plants displayed a noteworthy enhancement in activities of MDHAR (by 100.07 and 102.05%), DHAR (by 93.64 and 172.27%), and GR (by 150.85 and 207.43%, respectively); however, there were no noticeable differences in POD and APX activities between 'Ctrl', 'B1' and 'B2' plants (Fig. 7C–G). In comparison with 'Ctrl' plants, the activities of enzymatic GPX and GST were substantially improved by 79.98 and 35.83%, respectively, in 'As^V' plants (Fig. 7H, I). 'B1 + As^V' and 'B2 + As^V' maize plants demonstrated significantly improved activities of GPX by 25.37 and 138.19%, and GST by 61.48 and 153.83%, respectively, when contrasted with 'As^V' plants (Fig. 7H, I). Moreover, biochar applications to arsenic-devoid plants also displayed substantial improvement in the activities of GPX by 66.44 and 65.05%, and GST by 50.45 and 133.78%, in 'B1' and 'B2' plants, respectively, as compared with that of 'Ctrl' plants (Fig. 7H, I). On the other hand, total flavonoid contents significantly decreased by 50.27% in 'As^V' plants in relation to 'Ctrl' plants (Fig. 7J). Interestingly, 'B1 + As^V' and 'B2 + As^V' plants exhibited notable increase in total flavonoids content

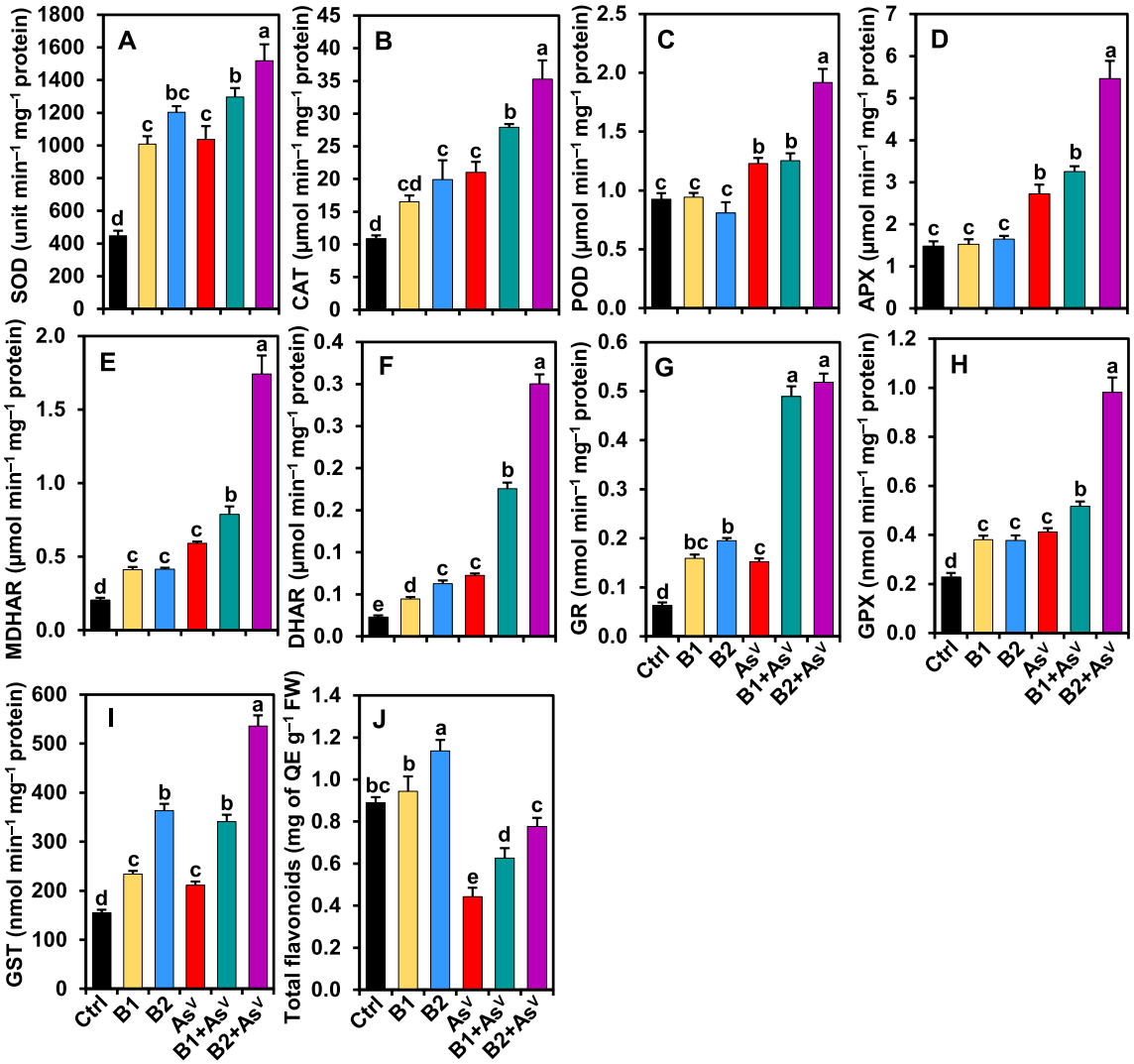

Fig. 7 Effect of biochar on the activities of enzymatic antioxidants (**A**) SOD, (**B**) CAT, (**C**) POD, (**D**) APX, (**E**)) MDHAR, (**F**) DHAR, (**G**) GR, (**H**) GPX, and (**I**) GST, and the levels of non-enzymatic antioxidant (**J**) total flavonoids in the leaves of maize plants subjected to sodium arsenate (Na_2AsO_4, As^V) stress for a period of nine days. Numerical data presented here indicate means ± standard errors of three biological repeats. LSD test determines the significant differences (at $P < 0.05$) between treatments by different alphabetical letters. Ctrl, B1, B2, As^V, B1 + As^V and B2 + As^V indicate 0 mg As^V Kg^{-1} soil, 2.5% biochar-added soil, 5.0% biochar-added soil, 100 mg As^V Kg^{-1} soil, 2.5% biochar-added soil + 100 mg As^V Kg^{-1} soil, and 5.0% biochar-added soil + 100 mg As^V Kg^{-1} soil, respectively. *APX* ascorbate peroxidase, *CAT* catalase, *DHAR* dehydroascorbate reductase, *FW* fresh weight, *GST* glutathione *S*-transferase, *GPX* glutathione peroxidase, *GR* glutathione reductase, *LSD* least significant difference, *MDHAR* monodehydroascorbate reductase, *POD* peroxidase, *QE* quercetin equivalent, *SOD* superoxide dismutase

by 41.48 and 75.37%, respectively, when compared with 'As^V' plants (Fig. 7J). Although we found no significant differences in total flavonoids level between 'Ctrl' and 'B1', 'B2' plants displayed an increase level of total flavonoids by 27.70%, relative to 'Ctrl' plants (Fig. 7J). These findings clearly demonstrated that enzymatic antioxidants SOD, CAT, POD, APX, MDHAR, DHAR, GR, GPX, and GST activity and the non-enzymatic antioxidant total flavonoids levels, responded favorably to the biochar pretreatments in As^V-stressed maize plants, with 'B2 + As^V' plants showed better performance than 'B1 + As^V' plants.

3.7 Application of biochar differentially maintained the levels of leaf RWC, Pro, TSS, TFAA, and total carbohydrate in As^V-stressed maize plants

When maize plants were exposed to arsenic stress, the level of leaf RWC, TFAA, and total carbohydrates were decreased by 30.49, 19.76, and 45.15%, and Pro and TSS content were increased by 125.96 and 62.70%,

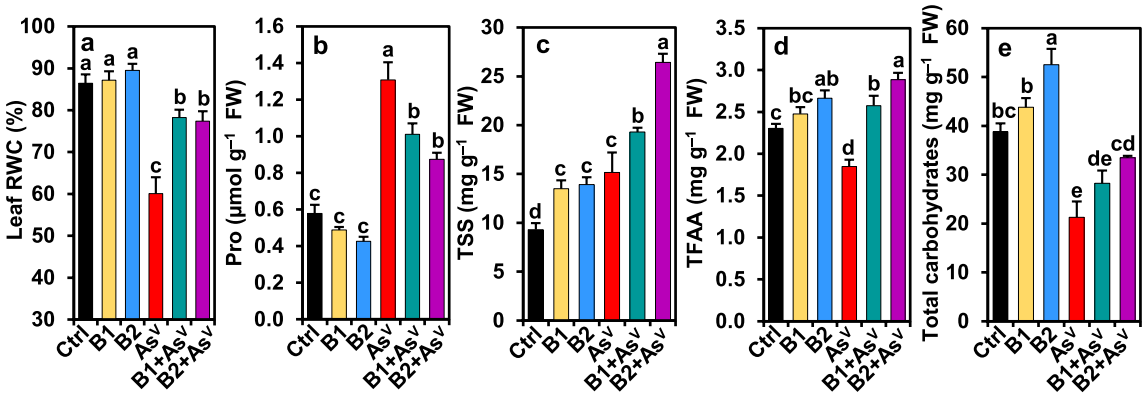

Fig. 8 Effect of biochar on the levels of (**a**) leaf RWC, (**b**) Pro, (**c**) TSS, (**d**) TFAA, and (**e**) total carbohydrates in maize plant leaves subjected to sodium arsenate (Na_2AsO_4, As^V) stress for a period of nine days. Numerical data presented here indicate means ± standard errors of three biological repeats. LSD test determines the significant differences (at $P < 0.05$) between treatments by different alphabetical letters. Ctrl, B1, B2, As^V, B1 + As^V and B2 + As^V indicate 0 mg As^V Kg^{-1} soil, 2.5% biochar-added soil, 5.0% biochar-added soil, 100 mg As^V Kg^{-1} soil, 2.5% biochar-added soil + 100 mg As^V Kg^{-1} soil, and 5.0% biochar-added soil + 100 mg As^V Kg^{-1} soil, respectively. *FW* fresh weight, *LSD* least significant difference, *Pro* proline, *RWC* relative water content, *TFAA* total free amino acids, *TSS* total soluble sugars

respectively, when compared with 'Ctrl' plants (Fig. 8A–E). Pretreatment of maize plants with biochar resulted in enhancement of leaf RWC (by 30.22 and 28.84%), TSS (27.34 and 74.42%), TFAA (39.30 and 56.09%), total carbohydrates (32.69% in 'B1 + As^V' plants), and decrement of Pro (by 22.70 and 33.21%) in 'B1 + As^V' and 'B2 + As^V' plants, respectively, relative to 'As^V' plants (Fig. 8A–E). In addition, compared with 'Ctrl' plants, 'B2' plants exhibited a significant enhancement in TFAA and total carbohydrates content by 15.57 and 35.29%, respectively, while both 'B1' and 'B2' plants showed a substantial improvement in the level of TSS by 44.95 and 49.39%, respectively (Fig. 8C–E). However, the level of leaf RWC and Pro did not differ significantly among 'Ctrl', 'B1', and 'B2' plants (Fig. 8A, B). These results suggested that biochar pretreatment resulted in greater accumulations of TSS, TFAA, and total carbohydrates in 'B2 + As^V' plants than in 'B1 + As^V' plants. Additionally, these results demonstrated that biochar treatment was effective in slowing the rise in Pro and balancing the leaf RWC in 'B1 + As^V' and 'B1 + As^V' plants.

3.8 Effects of biochar on the levels of mineral nutrients in the leaves and roots of As^V-stressed maize plants

In comparison with arsenic-free 'Ctrl' plants, K^+ content in leaves of 'As^V' plants significantly decreased by 42.69%; however, no significant divergence in K^+ content in roots was observed between 'Ctrl' and 'As^V' plants (Fig. 9A, E). In contrast, the addition of biochar significantly improved K^+ content in leaves of 'B1 + As^V' and 'B2 + As^V' plants by 126.06 and 384.52%, respectively, while the K^+ content in roots of 'B2 + As^V' plants increased by 123.23%, as compared with 'As^V' plants (Fig. 9A, E). Moreover, K^+ content in the leaves and roots of 'B2' plants was significantly increased by 28.03 and 145.12%, respectively, in contrast with 'Ctrl' plants (Fig. 9A, E). We did not observe any noteworthy variations of Ca^{2+} content in leaves between 'Ctrl' and 'As^V' plants; nevertheless, in roots, Ca^{2+} content significantly improved by 33.12% in 'As^V' plants, in relation to 'Ctrl' plants (Fig. 9B, F). In comparison with 'As^V' plants, Ca^{2+} content in leaves was increased by 21.41 and 26.20%, and in roots, decreased by 31.53 and 19.37%, in 'B1 + As^V' and 'B2 + As^V' plants, respectively (Fig. 9B, F). Although we did not observe any significant variations of Ca^{2+} content in leaves among 'Ctrl', 'B1', and 'B2' plants, Ca^{2+} content in roots was substantially improved by 15.75% in 'B1' and 'B2' plants, respectively, in relation to 'Ctrl' plants (Fig. 9B, F).

The Mg^{2+} content in leaves and roots did not differ significantly between 'Ctrl' and 'As^V' plants (Fig. 9C, G). Of interest, the addition of biochar substantially improved the Mg^{2+} content in leaves (by 180.03 and 261.78%), and roots (by 121.48 and 138.17%) in 'B1 + As^V' and 'B2 + As^V' plants, respectively, when compared to 'As^V' plants (Fig. 9C, G). We did not observe any significant divergence of Mg^{2+} content in leaves and roots between 'B1' and 'Ctrl' plants. However, 'B2' plants showed notable improvement of Mg^{2+} content in leaves and roots by 106.57 and 163.69%, respectively, when contrasted with 'Ctrl' plants (Fig. 9C, G). We did not observe any substantial variations of Fe^{2+} content in leaves and roots between 'Ctrl' and 'As^V' plants (Fig. 9D, H). Contrariwise, 'B1 + As^V' and 'B2 + As^V' plants displayed significant enhancement of Fe^{2+} content in roots by 84.12 and 160.91%, respectively, relative to 'As^V' plants, while no noteworthy variations were observed for Fe^{2+} content

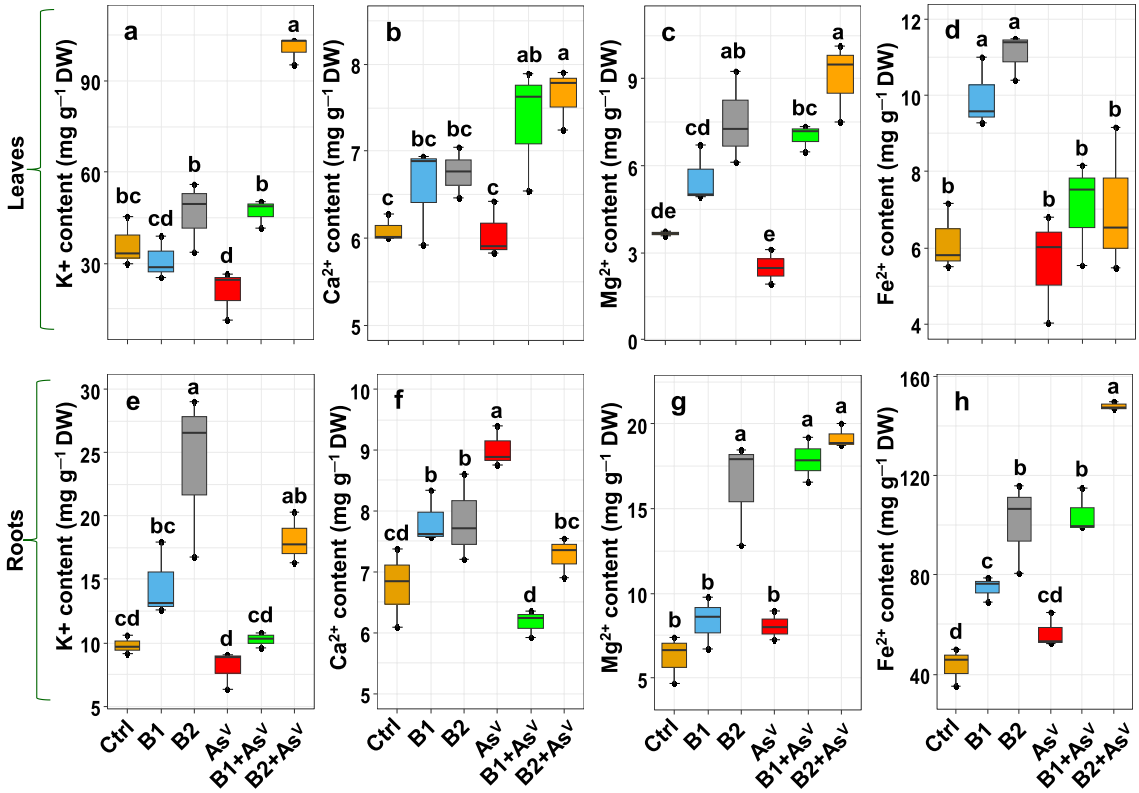

Fig. 9 Effect of biochar on the levels of (**a**, **e**) K^+, (**b**, **f**) Ca^{2+}, (**c**, **g**) Mg^{2+}, and (**d**, **h**) Fe^{2+} in leaves and roots, respectively of maize plants subjected to sodium arsenate (Na_2AsO_4, As^V) for a period of nine days. Numerical data presented here indicate means ± standard errors of three biological repeats. LSD test determines the significant differences (at $P < 0.05$) between treatments by different alphabetical letters. Ctrl, B1, B2, As^V, B1 + As^V and B2 + As^V indicate 0 mg As^V Kg^{-1} soil, 2.5% biochar-added soil, 5.0% biochar-added soil, 100 mg As^V Kg^{-1} soil, 2.5% biochar-added soil + 100 mg As^V Kg^{-1} soil, and 5.0% biochar-added soil + 100 mg As^V Kg^{-1} soil, respectively. *DW* dry weight, *LSD* the least significant difference

in leaves among 'As^V', '$B1 + As^V$', and '$B2 + As^V$' plants (Fig. 9D, H). In comparison with 'Ctrl' plants, 'B1' and 'B2' plants displayed a significant increase of Fe^{2+} content in leaves by 61.44 and 80.04% and in roots by 71.48 and 131.68%, respectively (Fig. 9D, H). The results suggested that under As^V stress conditions, biochar pretreatment positively stimulated the uptake of K^+, Ca^{2+}, Mg^{2+} in leaves and roots, and Fe^{2+} in roots only. The uptake seemed more prominent in '$B2 + As^V$' plants than '$B1 + As^V$' plants for all the mentioned minerals, while for Mg^{2+} in roots of '$B1 + As^V$' and '$B2 + As^V$' plants displayed similar results.

4 Discussion

Human and livestock exposure to arsenic through consumption of maize and maize-related products is a worldwide health concern. There is indeed an urgent need to either remediate arsenic-polluted maize soils or adapt strategies that could prevent arsenic accumulation in maize grains while maintaining better growth performance. Here, we demonstrate how biochar application contributes to mitigation of arsenic toxicity in maize plants grown under excessive As^V-stress conditions. We investigated biochar properties, as well as several physiological and biochemical mechanisms modulated by biochar applications to As^V-exposed maize plants. Our SEM image analysis revealed that rice husk biochar had an intricately uneven surface, which facilitated the metal absorption capacity (Fig. 2A–H). The concurrent presence of silica on the biochar surface substantially increased the retention of metal ions (Fig. 2N, Q). This was attributed to silica's role in pH regulation within soil, as well as its contribution to processes like metal co-precipitation and the creation of inorganic crystals in carbonaceous materials, serving as a mechanism to mitigate metal toxicity (Acharya et al. 2019). Notably, the biochar's near neutral pHzpc value of 6.8, uniquely facilitated the adsorption of both anions and cations, making rice husk biochar exceptionally effective for removing heavy metals, such as As^V from aqueous solutions without distorting other essential nutrient elements (Additional file 1: Fig. S3), which also aligned with the previous research findings of Samsuri et al. (2013).

Arsenic is a nonessential element for plants, as it does not play any positive role in normal plant growth and metabolism. Rather, evidence from multiple plant species, including soybean (*Glycine max*), rice (*Oryza sativa*), tomato (*Solanum lycopersicum*), and wheat (*Triticum aestivum*), suggests that a little accumulation of arsenic in plant cells can impede developmental processes, resulting in growth defects (Das et al. 2022; Hakeem et al. 2022; Jia-Yi et al. 2022; Kaya and Ashraf 2022; Li et al. 2022). Our findings also revealed that As^V-stress severely impacted maize growth, which was reflected through phenotype aberrations and reductions of plant height, leaf area, and biomass (Fig. 3A, B; Fig. 4A–F). The As^V-induced growth defects also positively correlated with enhanced As^V uptake in roots and aerial parts of the maize plants (Fig. 3C–E). These findings corroborated earlier studies and indicated that elevated levels of arsenic in roots and shoots of rice, wheat, and soybean are interlinked with the inhibition of roots and shoots growth, as well as reduction in biomass production (Das et al. 2022; Hakeem et al. 2022; Li et al. 2022). The current study also demonstrated that biochar addition to the soil restricted As^V uptake by maize roots, leading to a reduced accumulation of As^V in the aboveground part (Fig. 3C–E). The common mechanisms of biochar-mediated arsenic remediation from contaminated soils include improved electrostatic attraction, ion exchange process, surface sorption, complexation, and precipitation functions (Kumar et al. 2022; Liu et al. 2022b; Xu et al. 2022a). Furthermore, biochar can potentially aid in improvement of root structure, which facilitates water and nutrient acquisition from soils for improved growth of plants under arsenic stress conditions. Biochar-mediated decrease of As^V uptake and accumulation, as well as subsequent growth promotion, has also been observed in various plant species, including rice (Irshad et al. 2020) and cowpea (*Vigna unguiculata*) (Zhou et al. 2022).

Photosynthesis is the fundamental process required for carbon fixation and biomass accumulation in plants. Leaf Chl levels represent a vital indicator of photosynthetic performance of plants (Hou et al. 2020). Our present work revealed that As^V-stress declined the rate of P_n, E and g_s, as well as levels of photosynthetic pigments in maize leaves, which likely contributed to poor growth and biomass formation in As^V-stressed maize plants (Figs. 4A–F, 5A, B, D–H). Indeed, arsenic is well-recognized for its adverse impacts on photosynthesis, as evidenced by the disruption of chloroplast membranes, degradation of photosystem I and II (PSI and PSII), and hinderance or deactivation of enzymes essential to the dark phase, such as rubisco (Bano et al. 2022a; Chandrakar et al. 2018). Consistent with our findings, the As^V-induced attenuation of photosynthetic performance and degradation of photosynthetic pigments was also recorded in numerous crop plants, including tobacco (*Nicotiana sylvestris*) (Kofroňová et al. 2020). The improvement of gas-exchange features and photosynthetic pigments in biochar-supplemented As^V-stressed seedlings implied that biochar amendment may be associated with enhanced availability and retention of soil N, along with its subsequent utilization by the seedlings (Hou et al. 2020; Kamran et al. 2020; Wang et al. 2021). In addition, improvement of root growth in biochar-supplemented seedlings supports the notion of increased water and nutrient acquisition from the soil, which in turn stimulates plant photosynthesis and growth (He et al. 2020; Xiang et al. 2017).

A plethora of studies stated that accumulation of arsenic in plants is often associated with membrane disintegration, imbalanced cellular homeostasis, and even cell demise, predominantly by triggering oxidative stress and genotoxic effect of excessive ROS (Mostofa et al. 2021a, b; Mittler et al. 2022). Our results demonstrated that maize plant leaves generated large amounts of ROS ($O_2^{\bullet-}$ and H_2O_2) and MDA, along with high LOX activity in response to As^V-stress (Fig. 6A–E). These results implied that As^V exposure led to a state of oxidative stress, which manifested by increased levels of MDA and EL in As^V-stressed maize leaves. Biochar-treated plants, on the other hand, exhibited heightened resilience against As^V-stress, attributable to an enhanced regulation of oxidative damage, as indicated by diminished accumulation of ROS, and decreased level of MDA, LOX activity, and EL in maize leaves subjected to As^V-stress (Fig. 6A–F). Our results corroborated earlier studies that demonstrated the alleviating role of biochar in relieving oxidative stress induced by nickel in chili (*Capsicum frutescens*), arsenic in quinoa (*Chenopodium quinoa*), and cadmium in broad bean (*Vicia faba*) leaves (Helaoui et al. 2022; Shabbir et al. 2021; Turan 2022).

Next, we investigated the responses of ROS-detoxifying antioxidant defense system by examining the activities of several key antioxidant enzymes and levels of flavonoids in maize leaves subjected to both normal and As^V-stress conditions, with and without biochar treatment (Fig. 7A–J). Our findings clearly indicated that biochar-treated As^V-stressed plants effectively triggered ROS detoxification by boosting activities of SOD, which dismutated $O_2^{\bullet-}$ into H_2O_2, as well as CAT and POD, which convert H_2O_2 to H_2O (Fig. 7A–C) (Mostofa et al. 2021a, b; Mittler et al. 2022). APX, DHAR, GR, and MDHAR are the enzymes involved in the (AsA)-(GSH) cycle for eliminating H_2O_2. The AsA-GSH system also plays crucial roles in maintaining cellular redox balance by regenerating AsA and GSH, which is important for promoting heavy

metal stress tolerance in plants (Zulfiqar and Ashraf 2022). In this study, biochar-pretreated plants exposed to As^V-stress displayed higher activities of APX, DHAR, GR, and MDHAR when compared with As^V-stressed plants only, indicating positive effects of biochar on AsA-GSH cycle for enhancing H_2O_2 elimination (Figs. 6B,C, 7D–G). Additionally, the enhancement of MDHAR, DHAR, and GR activities also suggested a better maintenance of redox status in biochar-treated As^V-stressed maize leaves. More fundamentally, GSH-associated enzymes, including GPX and GST, use GSH as a cofactor to neutralize reactive aldehydes (Mittler et al. 2022). Intriguingly, biochar-pretreated As^V-stressed seedlings showed significantly higher GPX and GST activities than only As^V-stressed seedlings (Fig. 7H, I), suggesting that biochar protected maize plants from toxic aldehydes by activating these two enzymes (Fig. 6D). Flavonoids are well-known non-enzymatic antioxidants that protect oxidative damage to cell membrane integrity by directly quenching ROS during metalloid stresses (Anjitha et al. 2021; Flora 2009). In the current study, high levels of flavonoids in As^V-stressed plants supplemented with biochar implied that biochar addition aided maize plants in conferring protection against As^V-caused oxidative damage (Fig. 7J). Together, synergistic functions of enzymatic and non-enzymatic defense factors against ROS might have contribution to superior growth performance of maize plants treated with biochar under As^V-stress conditions.

Plants also accumulate low-molecular-weight compatible solutes like Pro, in addition to a robust antioxidant defense system, as part of adaptive mechanisms to maintain plant-water status under stressful conditions (Kumar et al. 2014; Moulick et al. 2016). Nevertheless, Pro accumulation is not always associated with stress tolerance (Mostofa et al. 2015; Mansour and Salama 2020). Numerous studies have asserted that increased levels of Pro correspond to the severity of stress symptoms when plants are subjected to various abiotic stresses (Khan et al. 2021; Mostofa et al. 2015; Rahman et al. 2022). In this study, we revealed that under As^V-stress, Pro and leaf RWC levels are reciprocally associated, whereas biochar supplementation restored RWC without accumulating much Pro (Fig. 8A, B). These results suggested that biochar addition was probably used for other metabolic adjustments, requiring a low level of Pro accumulation, which corroborated with the observed increase in total free amino acids and total soluble sugars levels (Fig. 8B–D). Several earlier studies have also found that total soluble sugars and total free amino acids played significant roles in maintaining the plant water status in response to abiotic stresses, including As^V-stress (Bano et al. 2022b; Sattar et al. 2022). Furthermore, increased levels of total soluble sugars and total free amino acids are known to guarantee a sufficient supply of nitrogen and carbon to better support plant metabolism under stressful circumstances (Ali et al. 2019; Rosa et al. 2009).

Because arsenic stress can severely impact plants' nutrient uptake mechanism, it is interesting to know whether biochar application has any ameliorating impact on nutrient absorption in maize plants under As^V-stress. Our results demonstrated that As^V-stressed maize plants accumulated less Ca^{2+} in leaves and less K^+, Mg^{2+}, and Fe^{2+} in both leaves and roots when compared with normal maize plants without As^V-stress (Fig. 9A–H). This observation may indicate As^V-mediated root damage and abnormal functions of ion channels embedded in the roots, which together led to a diminished capacity of nutrient absorption from soils (Figs. 3A, B, 9A–H) (Farhangi-Abriz and Ghassemi-Golezani 2022). In the presence of biochar, As^V-stressed maize plants exhibited enhanced uptake of K^+, Ca^{2+} (only in leaves), Mg^{2+}, and Fe^{2+} in their leaves and roots (Fig. 9A–H). Biochar itself serves as a reservoir of numerous macro and micronutrients, which gradually release upon integration in soils. This, in turn, increases the availability of nutrients to be utilized by roots followed by transportation and distribution to different plant organs (Farhangi-Abriz and Ghassemi-Golezani 2022). Furthermore, our findings revealed that biochar incorporation improved the root structure of maize plants (Fig. 3B) and possibly hydraulic conductivity and water retention in soil (Barnes et al. 2014; Wong et al. 2022), which aided nutrient absorption for sustaining plant growth under As^V-stress conditions. The biochar-induced high K^+ acquisition might play a crucial role in elevating rubisco activity, gas exchange in chloroplasts, and activation of several enzymes related to energy metabolism, protein synthesis, and solute transport (Mostofa et al. 2022). Ca^{2+} is known to regulate stomatal movement and the rate of photosynthetic electron transfer, whereas Fe^{2+} and Mg^{2+} are required for Chl biosynthesis in plants (Faizan et al. 2022; Singh et al. 2020; Therby-Vale et al. 2021; Wang et al. 2019). Thus, the greater photosynthetic rate and consequently, better growth performance was likely facilitated by biochar-mediated greater uptake of Ca^{2+}, Mg^{2+}, and Fe^{2+} in maize plants under As^V-stress conditions.

5 Conclusions

The current study provides a comprehensive understanding of biochar-mediated As^V -stress-resistance mechanisms in maize plants (Fig. 10). Biochar application potentially alleviated As^V-induced phytotoxicity by restricting As^V uptake and translocation, protecting photosynthetic apparatus and pigments, accumulating

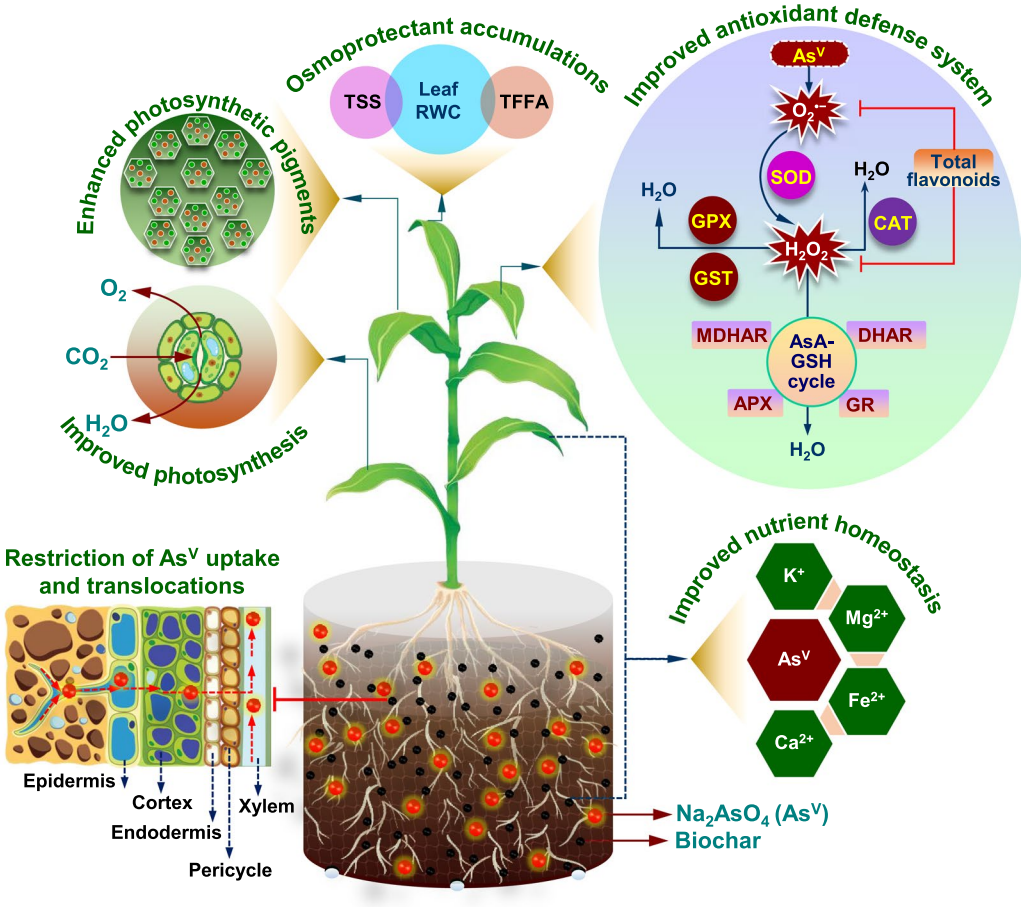

Fig. 10 Mechanisms involved in biochar-induced As^V-stress mitigation in maize plants. The addition of biochar to soil aids in the elimination of As^V from the soil through a variety of mechanisms, including adsorption; thus, restricting As^V uptake by roots and, as a result, lowering As^V translocation from roots to leaves. Biochar also increased the uptake of other mineral nutrients, such as K^+, Ca^{2+}, Mg^{2+}, and Fe^{2+}, which eventually aids in enhanced photosynthesis. Osmotic adjustment is further aided by the biochar-mediated buildup of osmoprotectants, such as total soluble sugars and total free amino acids. Importantly, the robust antioxidant defense system regulated by biochar, which includes both enzymatic and non-enzymatic antioxidants, aids in reducing the oxidative burden caused by As^V-stress. All of these contributed to better maize growth under As^V-stress

osmoprotectants, upregulating antioxidant defense system, and elevating the levels of mineral nutrients. These findings demonstrate the potential functions of biochar in modulating various physiological and biochemical pathways crucial for crop protection against arsenic stress. However, identification of molecular targets of biochar in maize might aid an in-depth understanding on how biochar can regulate plant defense mechanisms against excessive arsenic stress. Our study did not replicate the natural environment, therefore a field trial with a concurrent cost–benefit analysis would be necessary to verify the effectiveness of biochar as a low-cost technique for reducing As^V-induced negative impacts on maize growth and seed quality.

Supplementary Information

The online version contains supplementary material available at https://doi.org/10.1007/s42773-023-00270-6.

Additional file 1: Fig. S1. Phenotypic changes of maize plants subjected to different gradients of biochar for a period of twenty-five days. **Fig. S2.** Phenotypic changes of maize plants subjected to different gradients of sodium arsenate (Na_2AsO_4, As^V) stress for a period of twenty-five days. **Fig. S3.** Determination of the zero-point charge (pHzpc) of rice husk biochar. **Fig. S4.** Effects of biochar on maize phenotypes after exposure to As^V-stress for five days (A) and recovered from As^V-stress for five days (B). **Table S1.** The properties of biochar used in this study. **Table S2.** The chemical properties of soil after nine days of As^V-stress treatment. **Table S3.** Concentration of arsenic in soil and in biochar under different treatment combination after 9-days of stress treatment.

Acknowledgements
The authors express their gratitude to the Department of Soil Science at Bangabandhu Sheikh Mujibur Rahman Agricultural University in Gazipur,

Bangladesh, and the Pathology Division of Bangladesh Rice Research Institute, Gazipur, Bangladesh for granting access to their facilities. These facilities were utilized for the analysis of nutrient in soil and biochar, as well as for the characterization of Biochar using Scanning Electron Microscope (SEM).

Author contributions
MMR: conceptualization, methodology, writing-original draft preparation, writing-review and editing. MGM: conceptualization, methodology, writing-review and editing, supervision. LSPT: supervision. AKD, PKG, SS, MRI and SAIN: formal analysis and investigation. SSK and SMA: writing-original draft preparation. ML and PF: writing-review and editing. MAR, MARK and MA, and TRA: resources. All authors read and approved the final manuscript.

Funding
This research did not receive any specific grant from funding agencies in the public, commercial, or not-for-profit sectors.

Availability of data and materials
The datasets used or analyzed during the current study are available from the corresponding author on reasonable request.

Declarations

Competing interests
The authors declare that they have no known competing financial interests or personal relationships that could have appeared to influence the work reported in this paper.

Author details
[1]Department of Plant and Soil Science, Institute of Genomics for Crop Abiotic Stress Tolerance, Texas Tech University, Lubbock, TX 79409, USA. [2]Department of Agroforestry and Environment, Bangabandhu Sheikh Mujibur Rahman Agricultural University, Gazipur 1706, Bangladesh. [3]Institute of Biotechnology and Genetic Engineering (IBGE), Bangabandhu Sheikh Mujibur Rahman Agricultural University, Gazipur 1706, Bangladesh. [4]Department of Agronomy, Bangabandhu Sheikh Mujibur Rahman Agricultural University, Gazipur 1706, Bangladesh. [5]Plant Pathology Division, Bangladesh Rice Research Institute, Gazipur 1701, Bangladesh. [6]Department of Agriculture, Bangabandhu Sheikh Mujibur Rahman Science and Technology University, Gopalganj 8100, Bangladesh. [7]Department of Energy Plant Research Laboratory, Michigan State University, East Lansing, MI 48824, USA. [8]Plant Resilience Institute, Michigan State University, East Lansing, MI 48824, USA. [9]Department of Biochemistry and Molecular Biology, Michigan State University, East Lansing, MI 48824, USA.

Received: 25 January 2023 Revised: 12 October 2023 Accepted: 18 October 2023
Published online: 07 November 2023

References

Abbas G, Murtaza B, Bibi I, Shahid M, Niazi NK, Khan MI, Amjad M, Hussain M, Natasha (2018) Arsenic uptake, toxicity, detoxification, and speciation in plants: physiological, biochemical, and molecular aspects. Int J Environ Res Public Health 15:59. https://doi.org/10.3390/ijerph15010059

Acharya J, Kumar U, Meikap BC (2019) Thermodynamic spectral and kinetic analysis of the removal of Cu(II) from aqueous solution by sodium carbonate treated rice husk. J Environ Sci Health Part A 54:801–809. https://doi.org/10.1080/10934529.2019.1596699

Ahmed MF (2001) An overview of arsenic removal technologies in Bangladesh and India. In: Proceedings of BUET-UNU international workshop on technologies for arsenic removal from drinking water, Dhaka, pp 5–7

Ali I, Asim M, Khan TA (2013) Arsenite removal from water by electro–coagulation on zinc–zinc and copper–copper electrodes. Inter J Environ Sci Technol 10:377–384. https://doi.org/10.1007/s13762-012-0113-z

Ali Q, Athar H-R, Haider MZ et al (2019) Role of amino acids in improving abiotic stress tolerance to plants. In: Hasanuzzaman M, Fujita M, Oku H, Islam MT (eds) Plant tolerance to environmental stress. CRC Press, Boca Raton, pp 175–204. https://doi.org/10.1201/9780203705315-12

Alka S, Shahir S, Ibrahim N, Ndejiko MJ, Vo D-VN, Abd Manan F (2021) Arsenic removal technologies and future trends: a mini review. J Clean Prod 278:123805. https://doi.org/10.1016/j.jclepro.2020.123805

Anjitha KS, Sameena PP, Puthur JT (2021) Functional aspects of plant secondary metabolites in metal stress tolerance and their importance in pharmacology. Plant Stress 2:100038. https://doi.org/10.1016/j.stress.2021.100038

Arnon DI (1949) Copper enzyme in isolated chloroplasts: polyphenol oxidase in *Beta vulgaris*. Plant Physiol 24:1–15. https://doi.org/10.1104/pp.24.1.1

Bahrami A, Sathyapalan T, Moallem SA, Sahebkar A (2020) Counteracting arsenic toxicity: curcumin to the rescue? J Hazard Mater 400:123160. https://doi.org/10.1016/j.jhazmat.2020.123160

Bano K, Kumar B, Alyemeni MN, Ahmad P (2022a) Protective mechanisms of sulfur against arsenic phytotoxicity in *Brassica napus* by regulating thiol biosynthesis, sulfur-assimilation, photosynthesis, and antioxidant response. Plant Physiol Biochem 185:188–197. https://doi.org/10.1016/j.plaphy.2022.07.026

Bano K, Kumar B, Alyemeni MN, Ahmad P (2022b) Exogenously-sourced salicylic acid imparts resilience towards arsenic stress by modulating photosynthesis, antioxidant potential and arsenic sequestration in *Brassica napus* plants. Antioxidants 11:2010. https://doi.org/10.3390/antiox11102010

Barnes RT, Gallagher ME, Masiello CA, Liu Z, Dugan B (2014) Biochar-induced changes in soil hydraulic conductivity and dissolved nutrient fluxes constrained by laboratory experiments. PLoS ONE 9:e108340. https://doi.org/10.1371/journal.pone.0108340

Bates LS, Waldren RD, Teare ID (1973) Rapid determination of free proline for water stress studies. Plant Soil 39:205–207. https://doi.org/10.1007/BF00018060

Begum MC, Islam MS, Islam M, Amin R, Parvez MS, Kabir AH (2016) Biochemical and molecular responses underlying differential arsenic tolerance in rice (*Oryza sativa* L.). Plant Physiol Biochem 104:266–277. https://doi.org/10.1016/j.plaphy.2016.03.034

Ben Fredj F, Wali A, Khadhraoui M, Han J, Funamizu N, Ksibi M, Isoda H (2013) Risk assessment of heavy metal toxicity of soil irrigated with treated wastewater using heat shock proteins stress responses: case of El Hajeb, Sfax, Tunisia. Environ Sci Pollut Res 21:4716–4726. https://doi.org/10.1007/s11356-013-2411-5

Boyes S, Perera C, Young H (1992) Kiwifruit lipoxygenase, preparation and characteristics. J Food Sci 57:1390–1394. https://doi.org/10.1111/j.1365-2621.1992.tb06866.x

Bradford MM (1976) A rapid and sensitive method for the quantization of microgram quantities of protein utilizing the principle of protein–dye binding. Anal Biochem 72:248–254. https://doi.org/10.1016/0003-2697(76)90527-3

Chandrakar V, Pandey N, Keshavkant S (2018) Plant responses to arsenic toxicity: morphology and physiology. In: Hasanuzzaman M, Nahar K, Fujita M (eds) Mechanisms of arsenic toxicity and tolerance in plants. Springer, Singapore, pp 27–48. https://doi.org/10.1007/978-981-13-1292-2_2

Cheng N, Wang B, Wu P, Lee X, Xing Y, Chen M, Gao B (2021) Adsorption of emerging contaminants from water and wastewater by modified biochar: a review. Environ Pollut 273:116448

Das AK, Anik TR, Rahman MM, Keya SS, Islam MR, Rahman MA, Sultana S, Ghosh PK, Khan S, Ahamed T, Ghosh TK (2022) Ethanol treatment enhances physiological and biochemical responses to mitigate saline toxicity in soybean. Plants 11:272. https://doi.org/10.3390/plants11030272

De Feudis M, D'Amato R, Businelli D, Guiducci M (2019) Fate of selenium in soil: a case study in a maize (*Zea mays* L.) field under two irrigation regimes and fertilized with sodium selenite. Sci Total Environ 659:131–139. https://doi.org/10.1016/j.scitotenv.2018.12.200

Dixit G, Singh AP, Kumar A, Mishra S, Dwivedi S, Kumar S, Trivedi PK, Pandey V, Tripathi RD (2016) Reduced arsenic accumulation in rice (*Oryza sativa* L.) shoot involves sulfur mediated improved thiol metabolism, antioxidant system and altered arsenic transporters. Plant Physiol Biochem 99:86–96. https://doi.org/10.1016/j.plaphy.2015.11.005

Dubois M, Gilles KA, Hamilton JK, Rebers PA, Smith F (1956) Colorimetric method for determination of sugars and related substances. Anal Chem 28:350–356. https://doi.org/10.1021/ac60111a017

Faizan M, Bhat JA, El-Serehy HA, Moustakas M, Ahmad P (2022) Magnesium oxide nanoparticles (MGO-NPs) alleviate arsenic toxicity in soybean by modulating photosynthetic function, nutrient uptake and antioxidant potential. Metals 12:2030. https://doi.org/10.3390/met12122030
Farhangi-Abriz S, Ghassemi-Golezani K (2022) The modified biochars influence nutrient and osmotic statuses and hormonal signaling of mint plants under fluoride and cadmium toxicities. Front Plant Sci 13:5201. https://doi.org/10.3390/met12122030
Finnegan PM, Chen W (2012) Arsenic toxicity: The effects on plant metabolism. Front Physiol 3:1–18. https://doi.org/10.3389/fphys.2012.00182
Flora SJ (2009) Structural, chemical and biological aspects of antioxidants for strategies against metal and metalloid exposure. Oxidative Med Cell Longev 2:191–206. https://doi.org/10.4161/oxim.2.4.9112
Foyer CH, Halliwell B (1976) The presence of glutathione and glutathione reductase in chloroplasts: a proposed role in ascorbic acid metabolism. Planta 133:21–25. https://doi.org/10.1007/BF00386001
Gavrilescu M (2022) Enhancing phytoremediation of soils polluted with heavy metals. Curr Opin Biotechnol 74:21–31. https://doi.org/10.1016/j.copbio.2021.10.024
Hakeem KR, Alharby HF, Bamagoos AA, Pirzadah TB (2022) Biochar promotes arsenic (As) immobilization in contaminated soils and alleviates the astoxicity in soybean (*Glycine max* (L.) Merr.). Chemosphere 292:133407. https://doi.org/10.1016/j.chemosphere.2021.133407
Hasnat M, Alam MA, Khanam M, Binte BI, Kabir MH, Alam MS, Kamal MZ, Rahman GK, Haque MM, Rahman MM (2022) Effect of nitrogen fertilizer and biochar on organic matter mineralization and carbon accretion in soil. Sustainability 14:3684. https://doi.org/10.3390/su14063684
He Y, Yao Y, Ji Y, Deng J, Zhou G, Liu R, Shao J, Zhou L, Li N, Zhou X, Bai SH (2020) Biochar amendment boosts photosynthesis and biomass in C_3 but not C_4 plants: a global synthesis. GCB Bioenerg 12:605–617. https://doi.org/10.1111/gcbb.12720
Helaoui S, Boughattas I, Mkhinini M, El Kribi-Boukhris S, Livet A, Bousserhine N, Banni M (2022) Biochar improves the adaptability of *Vicia faba* L. in cadmium contaminated soil. Soil Sediment Contam 31:1–22. https://doi.org/10.1080/15320383.2022.2105811
Hossain MA, Nakano Y, Asada K (1984) Monodehydroascorbate reductase in spinach chloroplasts and its participation in the regeneration of ascorbate for scavenging hydrogen peroxide. Plant Cell Physiol 25:385–395. https://doi.org/10.1093/oxfordjournals.pcp.a076726
Hou Z, Tang Y, Li C, Lim KJ, Wang Z (2020) The additive effect of biochar amendment and simulated nitrogen deposition stimulates the plant height, photosynthesis and accumulation of NPK in pecan (*Carya illinoinensis*) seedlings. AoB Plants 12:plaa035. https://doi.org/10.1093/aobpla/plaa035
Hu Y, Boyer TH (2018) Removal of multiple drinking water contaminants by combined ion exchange resin in a completely mixed flow reactor. J Water Supply Res Technol AQUA 67:659–672. https://doi.org/10.2166/aqua.2018.101
IRRI (2021) Bangladesh and IRRI. http://books.irri.org/Bangladesh_IRRI_brochure.pdf
Irshad MK, Noman A, Alhaithloul HAS, Adeel M, Rui YK, Shah T, Zhu SH, Shang JY (2020) Goethite-modified biochar ameliorates the growth of rice (*Oryza sativa* L.) plants by suppressing Cd and As-induced oxidative stress in Cd and As co-contaminated paddy soil. Sci Total Environ 717:137086. https://doi.org/10.1016/j.scitotenv.2020.137086
Islam MR, Naznin T, Gupta DR, Haque MA, Hasanuzzaman M (2020) Insight into 5-aminolevulinic acid-induced modulation of cellular antioxidant metabolism to confer salinity and drought tolerance in maize. Biocell 44:713–730. https://doi.org/10.32604/biocell.2020.011812
Jackson ML (1973) Soil chemical analysis, (2nd Indian Print) Prentice-Hall of India Pvt. Ltd, New Delhi, 38–336
Jiang Z, Lian F, Wang Z, Xing B (2020) The role of biochars in sustainable crop production and soil resiliency. J Exp Bot 71:520–542. https://doi.org/10.1093/jxb/erz301
Jia-Yi Y, Meng-Qiang S, Zhi-Liang C, Yu-Tang X, Hang W, Jian-Qiang Z, Ling H, Qi Z (2022) Effect of foliage applied chitosan-based silicon nanoparticles on arsenic uptake and translocation in rice (*Oryza sativa* L.). J Hazard Mater 433:128781. https://doi.org/10.1016/j.jhazmat.2022.128781
Kamran M, Malik Z, Parveen A, Huang L, Riaz M, Bashir S, Mustafa A, Abbasi GH, Xue B, Ali U (2020) Ameliorative effects of biochar on rapeseed (*Brassica napus* L.) growth and heavy metal immobilization in soil irrigated with untreated wastewater. J Plant Growth Regul 39:266–281. https://doi.org/10.1007/s00344-019-09980-3
Kandhol N, Singh VP, Herrera-Estrella L, Tran LS, Tripathi DK (2022) Arsenite: the umpire of arsenate perception and responses in plants. Trends Plant Sci 27:420–422. https://doi.org/10.1016/j.tplants.2022.02.005
Kaya C, Ashraf M (2022) Sodium hydrosulfite together with silicon detoxifies arsenic toxicity in tomato plants by modulating the AsA-GSH cycle. Environ Pollut 294:118608. https://doi.org/10.1016/j.envpol.2021.118608
Khan Z, Khan MN, Zhang K, Luo T, Zhu K, Hu L (2021) The application of biochar alleviated the adverse effects of drought on the growth, physiology, yield and quality of rapeseed through regulation of soil status and nutrients availability. Ind Crop Prod 171:113878. https://doi.org/10.1016/j.indcrop.2021.113878
Kim TY, Ku H, Lee SY (2020) Crop enhancement of cucumber plants under heat stress by shungite carbon. Int J Mol Sci 21:4858. https://doi.org/10.3390/ijms21144858
Kofroňová M, Hrdinová A, Mašková P, Tremlová J, Soudek P, Petrová Š, Pinkas D, Lipavská H (2020) Multi-component antioxidative system and robust carbohydrate status, the essence of plant arsenic tolerance. Antioxidants 9:283. https://doi.org/10.3390/antiox9040283
Kumar A, Dwivedi S, Singh RP, Chakrabarty D, Mallick S, Trivedi PK, Adhikari B, Tripathi RD (2014) Evaluation of amino acid profile in contrasting arsenic accumulating rice genotypes under arsenic stress. Biol Plant 58:733–742. https://doi.org/10.1007/s10535-014-0435-4
Kumar A, Singh E, Mishra R, Kumar S (2022) Biochar as environmental armour and its diverse role towards protecting soil, water and air. Sci Total Environ 806:150444. https://doi.org/10.1016/j.scitotenv.2021.150444
Lee YP, Takahashi T (1966) An improved colorimetric determination of amino acids with the use of ninhydrin. Anal Biochem 14:71–77. https://doi.org/10.1016/0003-2697(66)90057-1
Li M, Song N, Song X, Liu J, Su B, Chen X, Guo X, Li M, Zong Q (2022) Investigating and modeling the toxicity of arsenate on wheat root elongation: assessing the effects of pH, sulfate and phosphate. Ecotoxicol Environ Saf 239:113633. https://doi.org/10.1016/j.ecoenv.2022.113633
Lichtenthaler K, Welburn AR (1983) Determination of total carotenoids and chlorophylls a and b of leaf extracts in different solvents. Biochem Soc Trans 11:591–592. https://doi.org/10.1042/bst0110591
Liu M, Almatrafi E, Zhang Y, Xu P, Song B, Zhou C, Zeng G, Zhu Y (2022a) A critical review of biochar-based materials for the remediation of heavy metal contaminated environment: applications and practical evaluations. Sci Total Environ 806:150531. https://doi.org/10.1016/j.scitotenv.2021.150531
Liu M, Zhu J, Yang X, Fu Q, Hu H, Huang Q (2022b) Biochar produced from the straw of common crops simultaneously stabilizes soil organic matter and heavy metals. Sci Total Environ 828:154494. https://doi.org/10.1016/j.scitotenv.2022.154494
Mansour MMF, Salama KHA (2020) Proline and abiotic stresses: responses and adaptation. In: Hasanuzzaman M (ed) Plant ecophysiology and adaptation under climate change: mechanisms and perspectives II. Springer, Singapore, pp 357–397
Mittler R, Zandalinas SI, Fichman Y, Van Breusegem F (2022) Reactive oxygen species signalling in plant stress responses. Nat Rev Mol Cell Biol 23:663–679. https://doi.org/10.1038/s41580-022-00499-2
Mostofa MG, Rahman A, Ansary MD, Uddin M, Watanabe A, Fujita M, Tran LS (2015) Hydrogen sulfide modulates cadmium-induced physiological and biochemical responses to alleviate cadmium toxicity in rice. Sci Rep 5:1–7. https://doi.org/10.1038/srep14078
Mostofa MG, Hossain MA, Siddiqui MN, Fujita M, Tran LS (2017) Phenotypical, physiological and biochemical analyses provide insight into selenium-induced phytotoxicity in rice plants. Chemosphere 178:212–223. https://doi.org/10.1016/j.chemosphere.2017.03.046
Mostofa MG, Ha CV, Rahman M, Nguyen KH, Keya SS, Watanabe Y, Itouga M, Hashem A, Abd-AllahFujitaHashem EFMLS (2021a) Strigolactones modulate cellular antioxidant defense mechanisms to mitigate arsenate toxicity in rice shoots. Antioxidants 10:1815. https://doi.org/10.3390/antiox10111815
Mostofa MG, Rahman MM, Nguyen KH, Li W, Watanabe Y, Tran CD, Zhang M, Itouga M, Fujita M, Tran LP (2021b) Strigolactones regulate arsenate uptake, vacuolar sequestration and antioxidant defense responses to

resist arsenic toxicity in rice roots. J Hazard Mater 415:125589. https://doi.org/10.1016/j.jhazmat.2021.125589
Mostofa MG, Rahman MM, Ghosh TK, Kabir AH, Abdelrahman M, Khan MAR, Mochida K, Tran LSP (2022) Potassium in plant physiological adaptation to abiotic stresses. Plant Physiol Biochem 186:279–289. https://doi.org/10.1016/j.plaphy.2022.07.011
Moulick D, Ghosh D, Santra SC (2016) Evaluation of effectiveness of seed priming with selenium in rice during germination under arsenic stress. Plant Physiol Biochem 109:571–578. https://doi.org/10.1016/j.plaphy.2016.11.004
Nakano Y, Asada K (1981) Hydrogen peroxide is scavenged by ascorbate-specific peroxidase in spinach chloroplasts. Plant Cell Physiol 22:867–880. https://doi.org/10.1093/OXFORDJOURNALS.PCP.A076232
Peña-Garcia Y, Shinde S, Natarajan P, Lopez-Ortiz C, Balagurusamy N, Chavez AC, Saminathan T, Nimmakayala P, Reddy UK (2021) Arsenic stress-related F-Box (ASRF) gene regulates arsenic stress tolerance in *Arabidopsis thaliana*. J Hazard Mater 407:124831. https://doi.org/10.1016/j.jhazmat.2020.124831
Piper CS (1966) Soil and plant analysis, Hans Pub, Bombay. Asian Ed, pp 368–374
Podgorski J, Berg M (2020) Global threat of arsenic in groundwater. Science 368:845–850. https://doi.org/10.1126/science.aba1510
Qiu B, Tao X, Wang H, Li W, Ding X, Chu H (2021) Biochar as a low-cost adsorbent for aqueous heavy metal removal: a review. J Anal Appl Pyrol 155:105081. https://doi.org/10.1016/j.jaap.2021.105081
Rahaman MS, Mise N, Ichihara S (2022) Arsenic contamination in food chain in Bangladesh: a review on health hazards, socioeconomic impacts and implications. Hyg Environ Health Adv 2:100004
Rahman MM, Mostofa MG, Islam M, Keya SS, Das AK, Miah M, Kawser AQ, Ahsan SM, Hashem A, Tabassum B, Abd-Allah EF (2019) Acetic acid: a cost-effective agent for mitigation of seawater-induced salt toxicity in mung bean. Sci Rep 9:1–15. https://doi.org/10.1038/s41598-019-51178-w
Rahman MM, Mostofa MG, Das AK, Anik TR, Keya SS, Ahsan SM, Khan MA, Ahmed M, Rahman MA, Hossain MM (2022) Ethanol positively modulates photosynthetic traits, antioxidant defense and osmoprotectant levels to enhance drought acclimatization in soybean. Antioxidants 11:516. https://doi.org/10.3390/antiox11030516
Rashid MS, Liu G, Yousaf B, Song Y, Ahmed R, Rehman A (2022) Efficacy of rice husk biochar and compost amendments on the translocation, bioavailability, and heavy metals speciation in contaminated soil: role of free radical production in maize (*Zea mays* L.). J Clean Prod 330:129805. https://doi.org/10.1016/j.jclepro.2021.129805
Rizvi A, Ahmed B, Khan MS, Rajput V, Umar S, Minkina T, Lee J (2022) Maize associated bacterial microbiome linked mitigation of heavy metal stress: a multidimensional detoxification approach. Environ Exp Bot 200:104911. https://doi.org/10.1016/j.envexpbot.2022.104911
Romdhane L, Panozzo A, Radhouane L, Dal Cortivo C, Barion G, Vamerali T (2021) Root characteristics and metal uptake of maize (*Zea mays* L.) under extreme soil contamination. Agronomy 11:178. https://doi.org/10.3390/agronomy11010178
Rosa M, Prado C, Podazza G, Interdonato R, González JA, Hilal M, Prado FE (2009) Soluble sugars: metabolism, sensing and abiotic stress: a complex network in the life of plants. Plant Signal Behav 4:388–393. https://doi.org/10.4161/psb.4.5.8294
Roy S, Sarkar D, Datta R, Bhattacharya SS, Bhattacharyya P (2022) Assessing the arsenic-saturated biochar recycling potential of vermitechnology: insights on nutrient recovery, metal benignity, and microbial activity. Chemosphere 286:131660. https://doi.org/10.1016/j.chemosphere.2021.131660
Samsuri AW, Sadegh-Zadeh F, Seh-Bardan BJ (2013) Sorption of As(III) and As(V) by Fe coated biochars and biochars produced from empty fruit bunch and rice husk. J Environ Chem Eng 1:981–988. https://doi.org/10.1016/j.jece.2013.08.009
Sattar A, Sher A, Abourehab MA, Ijaz M, Nawaz M, Ul-Allah S, Abbas T, Shah AN, Imam MS, Abdelsalam NR, Hasan ME (2022) Application of silicon and biochar alleviates the adversities of arsenic stress in maize by triggering the morpho-physiological and antioxidant defense mechanisms. Front Environ Sci 10:2086. https://doi.org/10.3389/fenvs.2022.979049
Senn AC, Hug SJ, Kaegi R, Hering JG, Voegelin A (2018) Arsenate co-precipitation with Fe(II) oxidation products and retention or release during precipitate aging. Water Res 131:334–345. https://doi.org/10.1016/j.watres.2017.12.038
Shabbir A, Saqib M, Murtaza G, Abbas G, Imran M, Rizwan M, Naeem MA, Ali S, Javeed HM (2021) Biochar mitigates arsenic-induced human health risks and phytotoxicity in quinoa under saline conditions by modulating ionic and oxidative stress responses. Environ Pollut 287:117348. https://doi.org/10.1016/j.envpol.2021.117348
Singh R, Parihar P, Prasad SM (2020) Interplay of calcium and nitric oxide in improvement of growth and arsenic-induced toxicity in mustard seedlings. Sci Rep 10:1–12. https://doi.org/10.1038/s41598-020-62831-0
Somogyi MJ (1952) Notes on sugar determination. J Biol Chem 195:19–23. https://doi.org/10.1016/S0021-9258(19)50870-5
Srivastav AL, Pham TD, Izah SC, Singh N, Singh PK (2021) Biochar adsorbents for arsenic removal from water environment: a review. Bull Environ Contam Toxicol 108:616–628. https://doi.org/10.1007/s00128-021-03374-6
Srivastava S, Srivastava AK, Sablok G, Deshpande TU, Suprasanna P (2015) Transcriptomics profiling of Indian mustard (*Brassica juncea*) under arsenate stress identifies key candidate genes and regulatory pathways. Front Plant Sci 6:646. https://doi.org/10.3389/fpls.2015.00646
Sun Y, Wang T, Bai L, Han C, Sun X (2022) Application of biochar-based materials for remediation of arsenic contaminated soil and water: preparation, modification, and mechanisms. J Environ Chem Eng 10:108292. https://doi.org/10.1016/j.jece.2022.108292
Therby-Vale R, Lacombe B, Rhee SY, Nussaume L, Rouached H (2021) Mineral nutrient signaling controls photosynthesis: focus on iron deficiency-induced chlorosis. Trends Plant Sci 27:502–509. https://doi.org/10.1016/j.tplants.2021.11.005
Turan V (2022) Calcite in combination with olive pulp biochar reduces Ni mobility in soil and its distribution in chili plant. Int J Phytoremediat 24:166–176. https://doi.org/10.1080/15226514.2021.1929826
Vezza ME, Luna DF, Agostini E, Talano MA (2019) Glutathione, a key compound for as accumulation and tolerance in soybean plants treated with AsV and AsIII. Environ Exp Bot 162:272–282. https://doi.org/10.1016/j.envexpbot.2019.03.002
Walkley A, Black IA (1934) An examination of the Degtjareff method for determining soil organic matter and a proposed modification of the chromic acid titration method. Soil Sci 37:29–38. https://doi.org/10.1097/00010694-193401000-00003
Wang Q, Yang S, Wan S, Li X (2019) The significance of calcium in photosynthesis. Int J Mol Sci 20:1353. https://doi.org/10.3390/ijms20061353
Wang S, Zheng J, Wang Y, Yang Q, Chen T, Chen Y, Chi D, Xia G, Siddique KH, Wang T (2021) Photosynthesis, chlorophyll fluorescence, and yield of peanut in response to biochar application. Front Plant Sci 12:650432. https://doi.org/10.3389/fpls.2021.650432
Wang R, Sun L, Zhang P, Wan J, Wang Y, Xu J (2022) Zinc oxide nanoparticles alleviate cadmium stress by modulating plant metabolism and decreasing cadmium accumulation in *Perilla frutescents*. Plant Growth Regul 23:1–2. https://doi.org/10.1007/s10725-022-00938-2
Wong JT, Chow KL, Chen XW, Ng CW, Wong MH (2022) Effects of biochar on soil water retention curves of compacted clay during wetting and drying. Biochar 4:1–4. https://doi.org/10.1007/s42773-021-00125-y
Xiang Y, Deng Q, Duan H, Guo Y (2017) Effects of biochar application on root traits: a meta-analysis. GCB Bioenergy 9:1563–1572. https://doi.org/10.1111/gcbb.12449
Xu Q, Xu Q, Zhu H, Li H, Yin W, Feng K, Wang S, Wang X (2022a) Does biochar application in heavy metal-contaminated soils affect soil micronutrient dynamics? Chemosphere 290:133349. https://doi.org/10.1016/j.chemosphere.2021.133349
Xu M, Xu M, Yang L, Chen Y, Jing H, Wu P, Yang W (2022b) Selection of rice and maize varieties with low cadmium accumulation and derivation of soil environmental thresholds in karst. Ecotoxicol Environ Saf 247:114244. https://doi.org/10.1016/j.ecoenv.2022.114244
Yan A, Wang Y, Tan SN, Mohd Yusof ML, Ghosh S, Chen Z (2020) Phytoremediation: A promising approach for revegetation of heavy metal-polluted land. Front Plant Sci 11. https://doi.org/10.3389/fpls.2020.00359
Yin Z, Zhang Y, Hu N, Shi Y, Li T, Zhao Z (2021) Differential responses of 23 maize cultivar seedlings to an arbuscular mycorrhizal fungus when grown in a metal-polluted soil. Sci Total Environ 789:148015. https://doi.org/10.1016/j.scitotenv.2021.148015
Yu CW, Murphy TM, Lin CH (2003) Hydrogen peroxide-induces chilling tolerance in mung beans mediated through ABA-independent glutathione

accumulation. Funct Plant Biol 30:955–963. https://doi.org/10.1071/FP03091

Zama EF, Li G, Tang YT, Reid BJ, Ngwabie NM, Sun GX (2022) The removal of arsenic from solution through biochar-enhanced precipitation of calcium-arsenic derivatives. Environ Pollut 292:118241. https://doi.org/10.1016/j.envpol.2021.118241

Zheng L, Li Y, Shang W, Dong X, Tang Q, Cheng H (2019) The inhibitory effect of cadmium and/or mercury on soil enzyme activity, basal respiration, and microbial community structure in coal mine-affected agricultural soil. Ann Microbiol 69:849–859. https://doi.org/10.1007/s13213-019-01478-3

Zhou J, Liu Y, Li B, Huang W, Qin J, Li H, Chen G (2022) Hydrous zirconium oxide modified biochar for in situ remediation of arsenic contaminated agricultural soil. J Environ Chem Eng 10:108360. https://doi.org/10.1016/j.jece.2022.108360

Zulfiqar F, Ashraf M (2022) Antioxidants as modulators of arsenic-induced oxidative stress tolerance in plants: an overview. J Hazard Mater 427:127891. https://doi.org/10.1016/j.jhazmat.2021.127891